Biomaterials Science

ROYAL SOCIETY OF CHEMISTRY

REVIEW

View Article Online
View Journal | View Issue

Cite this: *Biomater. Sci.*, 2026, **14**, 2237

Rational design of lipid and lipid-like structures for non-liver-targeted mRNA therapy

Yingwei Tang,[a] Di Li,[a] Yalin Zhu,[a] Hongwei Duan *[a] and Anshun Zhao*[b]

Received 4th September 2025,
Accepted 23rd March 2026

DOI: 10.1039/d5bm01344e

rsc.li/biomaterials-science

The application of mRNA therapies has witnessed significant advancement since the outbreak of COVID-19. However, the widespread use of mRNA therapies has been restricted by the liver accumulation of traditional lipid structures used as delivery vectors. The efficacy of mRNA expression has been demonstrated to be highly related to vector structures and properties. To expand non-liver organs or cells as therapeutic targets for mRNA, lipid and other lipid-like molecules such as lipid analogs and lipid-like polymers with more favorable mRNA delivery efficiencies have been developed based on a deeper understanding of their structure–function correlations. This review primarily summarizes the structure commonalities leading to an excellent delivery performance and specific organ or cell targeting and illustrates the potential and future prospects of related materials in different biomedical applications of mRNA therapies.

1 Introduction

Messenger RNA (mRNA)-based therapy has emerged as a promising avenue to address the limitations of traditional treatments for incurable diseases.[1,2] The prominent superiority of mRNA therapy is its capacity to drive precise and durable protein translation directly in the cytoplasm, bypassing the need to enter the nucleus, which eliminates the risk of random genome integration and enhances genetic safety.[3,4] Meanwhile, mRNA undergoes rapid degradation in the intracellular environment after protein expression to reduce its impact on the internal environment.[5] The COVID-19 pandemic has brought mRNA therapy into the spotlight to accelerate its development in clinical settings and industry. As a single-stranded ribonucleic acid, mRNA can be readily transcribed from a DNA template and produced on a large scale by *in vitro* transcription (IVT) technology, enabling standardized manufacturing with minimal impurities and reduced risk of viral contamination.[6] However, mRNA demonstrates inherent instability within the human body due to its quick hydrolysis by the nucleases rich in serum and the intracellular environment.[7] The intrinsic negative charge of mRNA further hinders its interaction with the cell membrane, limiting its efficient cell uptake to initiate protein translation.[5] Various delivery systems have been designed to protect mRNA throughout its *in vivo* journey to maintain the mRNA activity and ensure its safe delivery to the target site. Lipid nanoparticles (LNPs) have been found to be the most advanced non-viral system currently employed for mRNA delivery.[8–10] LNP systems generally consist of cationic/ionizable lipids, phospholipids, cholesterol, and PEG lipids.[11,12] Cationic/ionizable lipids play the predominant role in combining with mRNA,[13,14] and the *in vivo* destiny of mRNA is collectively influenced by the structural properties of all these lipid components.[15] At the same time, other materials imitating lipid structures are also under development, such as lipid analog molecules[16,17] and polymers.[18,19] These lipid-like materials contain the essential components of fundamental lipid structures, with additional functional groups integrated to fine-tune their properties. It can be found that some analogous structural features observed in lipids, lipid analogs, and lipid-like polymers exhibit common properties in terms of their *in vivo* behaviors, including targeting ability, cellular uptake, and endosomal escape. This emphasizes the existence of a structure–function relationship, which enables the regulation of the *in vivo* fate of mRNA through a combination of specific structures in lipid-like molecules.[20] Due to the strong liver tropism of conventional LNPs, the applicability of mRNA therapies for diseases in non-hepatic organs is highly limited.[21] Proper modulation of lipid structure has been widely utilized to promote targeted mRNA accumulation in non-liver organs and cells of interest in recent studies.[22] Understanding the relationship between structural features and targeting capabilities of carriers can streamline carrier composition, eliminate the need for complex synthetic modifications, and precisely identify effective ligands to achieve higher targeting accuracy. Current research studies have increasingly focused on understanding the detailed structure–

[a]*School of Chemistry, Chemical Engineering and Biotechnology, Nanyang Technological University, 70 Nanyang Drive, Singapore 637457, Singapore. E-mail: hduan@ntu.edu.sg*
[b]*Henan Key Laboratory of Cancer Epigenetics, The First Affiliated Hospital, College of Clinical Medicine, Henan University of Science and Technology, Luoyang, 471003, China. E-mail: anshunzhao@haust.edu.cn*

function relationship and elucidating the mechanisms underlying the changes in mRNA delivery performance. In this review, we aim to provide a primary overview of the structure–function relationships of lipid and lipid-like molecules in mRNA-targeted delivery reported in the latest research studies. We highlight the impact of key components in lipid and lipid-like structures on vector properties, as well as the material characteristics and design strategies that enable successful targeting of different non-liver organs for diverse biomedical applications (Fig. 1), serving as a reference for the rational design of these structures.

2 Structure–function relationship of lipid and lipid-like molecules

Generally, lipids that serve as mRNA carriers contain 3 components: a hydrophilic head group, hydrophobic tail, and linker group. Head groups produce positive charge to combine with negative-charged mRNA *via* electrostatic interaction and determine the pK_a of lipid molecules, which further affects the physicochemical characterization, immunogenicity, transfection efficiency, and *in vivo* distribution behavior of mRNA-LNP. The ionization degree and surface charge of LNPs are greatly controlled by the systemic apparent pK_a value.[23] As Jayaraman[24] and Hassett[25] have affirmed, the optimal pK_a value for the intravenous delivery of mRNA is between 6.2 and 6.5, while the ideal pK_a range for intramuscular delivery is between 6.6 and 6.9. When the pK_a is around 6–7, the LNPs display excellent transfection efficiency in the liver, and the apolipoprotein E (ApoE) adhering on the LNP surface when it moves through blood vessels also endows LNPs with strong liver tropism. However, it is reported that a pK_a out of normal range may induce an alteration in the biodistribution of LNPs to achieve targeted delivery to other organs.[26] For example, the LNPs with a pK_a more than 9 exhibit obvious lung-targeting ability, while LNPs with strong spleen tropism display a lower pK_a between 2–6.[27] Therefore, a wider range of pK_a can be considered when researchers design lipids and other lipid-like molecules, which allows more non-traditional chemical groups to be applied in lipid structures, especially lipid design for targeted delivery. Although the head group structures dominate the pK_a value, hydrophobic tail structures also can influence the properties[15] of lipid molecules, and some components affecting the surface charge can be added to LNPs to regulate their biological performance. In conclusion, the chemical structure of LNP components plays a critical role in determining the basic properties and targeting ability of LNPs. Regarding the design of lipid-like polymers used as mRNA carriers, more factors should be taken into consideration in addition to the structure–function relationship of typical lipids.

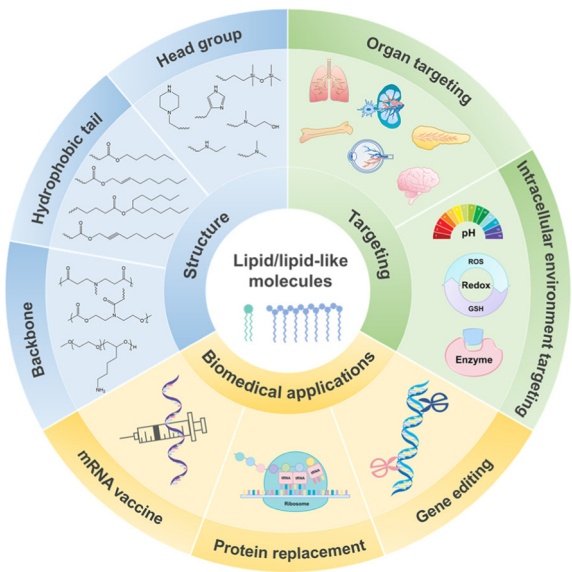

Fig. 1 Schematic of the lipid and lipid-like structures mediating non-liver organs and specific cell environment targeted delivery of mRNA and related biomedical applications.

2.1 Lipid/lipid analogs

2.1.1 Head group. Usually, amine head groups can be classified as primary, secondary, and tertiary amine in typical lipid structures, and more diversified head group structures such as quaternary amine, heterocyclic, and hydroxylamine have been extensively applied in the design of lipids to improve the performance of LNPs in mRNA delivery recently, indicating an essential relationship between head amine structure and lipid properties. Tesei *et al.*[28] performed an investigation on the interplay between head group size and lipid charge state. When the lipid was complexed with mRNA in the form of LNP, the ionization state of the amine group was greatly affected by the local environment, including the head groups of other lipid molecules, loaded mRNA and salt ions.[29] Therefore, the size-dependent ionization behaviors of amine head groups were explored under different environments utilizing computer simulation and NMR. Lipids featuring a smaller head group size were proven to maintain tight packing *via* electrostatics at a low pH and adopt a more disordered phase under deprotonated conditions, implying more efficient endosomal escape of loaded mRNA compared with larger-sized head groups.

The existence of other functional groups in the head group also contributes to the *in vivo* behaviors of LNPs and shows greater potential in LNP property improvement than a simple amine head group. Hydrogen bond-forming structures and heterocyclic structures are two known examples of such applications in lipids in recent studies. It has been found that some lipids exhibit an excellent delivery efficiency in the clinical COVID-19 mRNA vaccine, such as ALC-0315 and SM-102, both possessing a hydroxyl structure in their head group.[30] Similarly, Sabnis *et al.*[31] synthesized a series of lipids with an ethanolamine head group and found that they exhibit a superior transfection efficiency than the typical lipid DLin-MC3-DMA. Notably, replacing the head hydroxyl group with di-

methylamine completely degraded the mRNA delivery efficiency of these lipids. This loss of function was hypothesized to result from the ability of the hydroxyl group to form hydrogen bonds with mRNA for *in vivo* expression enhancement. Building on this finding, a follow-up study conducted by Cornebise *et al.*[32] further explored the structure–activity relationship of lipids based on other hydrogen bond-forming groups, as the alternatives to mimic the hydroxyl group efficacy (Fig. 2D). By altering the lipid head groups with diverse hydrogen-bond donors and acceptors, they conducted molecular dynamics simulations for the specific interactions between the backbone/nucleobase of mRNA and head groups of six lipids. Subsequently, *in vivo* assessments were performed and lipids with a squaramide group and thiourea group identified as the most effective ones for mRNA transfection (Fig. 2E), likely due to their increased hydrogen-bond donor capabilities and favorable π-stacking interactions. Owing to these characteristics, electrostatic interactions are not the only force to assemble LNPs and mRNA, which may contribute to a reduced reliance on PEG to control the size and stability of LNPs, and further improve their *in vivo* performance by decreasing the complement activation-related pseudoallergy (CARPA) generated from anti-PEG antibody.

Meanwhile, heterocyclic structures within the amine head groups of lipids have been reported to be implicated in modulating the immunogenicity of LNPs and inhibiting the production of anti-PEG antibodies in recent studies.[33] Chaudhary *et al.*[33] reported a potential structure-immune response relationship of lipids based on the interaction between the lipid amine head group and the TLR4 receptors (Fig. 2A). Among the different amine head groups in their library, heterocyclic structures induced a stronger increase in pro-inflammatory cytokines (Fig. 2B and C) and related immune response, exhibiting higher binding affinity with immune receptors. This head group structure-receptor affinity could be further simulated computationally to systemically predict the innate immunogenicity of LNPs. As mentioned above, the heterocyclic head group also caused relatively less production of anti-PEG lgM antibodies to reduce efficacy loss. Li *et al.*[34] also proved that a heterocyclic amine head structure could enhance the immunostimulatory properties of lipids. To serve as an immune adjuvant in an LNP-based mRNA vaccine, they synthesized a series of heterocyclic lipids that displayed excellent transfection activity and immunostimulatory, relatively addressing the insufficient immunity induced by mRNA alone. The findings from these studies suggest the application potential of lipids with heterocyclic-structured head domains, especially in mRNA vaccine carriers. One of the possible mechanisms for the immunocompetence of heterocyclic lipids may be a similar binding mode as TLR4 ligands to interact with the TLR4 amino acid residue for stimulation, as investigated by Chaudhary.[33] Evidently, the mechanism based on

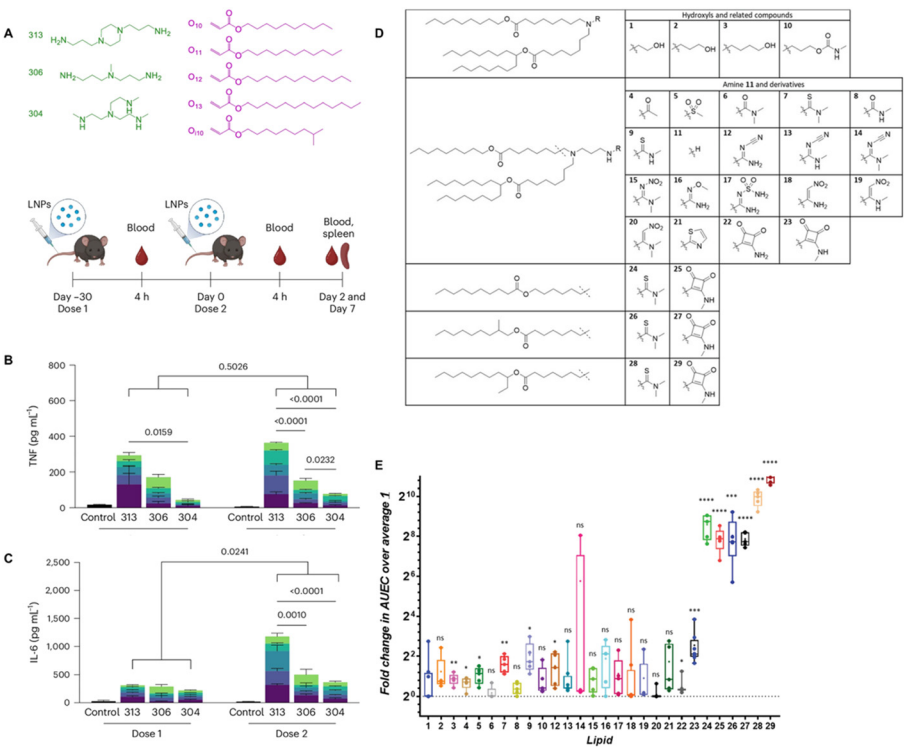

Fig. 2 (A) Combination lipid library of three amine headgroups (including heterocyclic group) and five acrylate tails. At 4 h after each dose, the inflammatory cytokines TNF (B) and IL-6 (C) were measured in the serum. Reprinted with permission from ref. 33. Copyright 2024, Springer Nature. (D) Structures of amino lipids with different hydrogen bond-containing groups. (E) Fold change in the hEPO mRNA expression AUEC of novel LNPs *versus* lipid 1 LNPs measured in CD-1 mice. Reprinted with permission from ref. 32. Copyright 2021, Wiley-VCH.

Toll-like receptors (TLR) is not universally applicable to all heterocyclic structures. The study of Miao *et al.*[35] demonstrated that lipids with cyclic structures also had the capacity to activate the STING pathway for the immune response and antitumor efficacy enhancement of an mRNA vaccine. However, further research is still needed to extend the understanding of the correlation between lipid headgroup chemistry and immunostimulatory mechanism.

Building on the above-mentioned studies, the structure–function relationship based on head group shows a more significant and precise regulation of lipid performance than expected. Therefore, regarding endowing lipids with targeting capacity, the ingenious design of head group structure can be emphasized. For example, Xue *et al.*[36] introduced a siloxane moiety into an amine head to enhance the intracellular uptake of LNPs. Notably, when the lipid head domain underwent minor structural alteration, the organ tropism of LNPs exhibited an apparent difference. It was found that substituting an ester bond with an amine bond in the siloxane head group switched the targeting from the liver to the lungs, and attaching a negatively charged sulfonic group in the siloxane moiety obviously facilitated spleen tropism. This example revealed that head group chemistry strongly influenced the targeting properties of LNPs, and not only their basic physicochemical characteristics, but also their deeper interaction mechanisms with the immune system and organs, and a detailed extension and classification of this topic will be provided in later sections.

2.1.2 Hydrophobic tail. The hydrophobic tail structures play a vital role in the shape control of lipids.[37] Typically, lipids with 2 hydrophobic chains can form a cone-like shape in the protonated state when exposed to the acidic environment of endosomes after cellular uptake and further combine with negatively charged membrane lipids, inversing the hexagonal phase (HII) to facilitate their following endosome/lysosome escape and mRNA release.[38] The formation of an inverse hexagonal phase, related intracellular behaviors, and biological efficacy of lipids are highly associated with the length, functional groups, and branched state of their hydrophobic tail. Traditional lipids generally contain 1–4 hydrophobic chains with a carbon length of 8 to 20 atoms.[39] The optimal tail length for lipids was reported to typically range between 12 and 14 carbon atoms[40] and it was found that the transfection efficiency declined when the tail length increased from 14 carbon atoms to 18 carbon atoms.[41] Furthermore, the functional groups within the hydrophobic tail, such as unsaturated groups (alkene bond and alkyne bond), ester bond, and amide bond, contribute more to the improvement in the properties of lipids for a better delivery efficiency. Unsaturated groups in the lipid tail are commonly perceived to enhance the membrane fluidity and lead to more effective endosome escape of the loaded mRNA.[42] Miao *et al.*[43] modified the backbone of Dlin-MC3-DMA with alkene, alkyne, and ester bonds in its tail structure to facilitate endosomal escape and systemic tolerability. They synthesized a series of alkene/alkyne lipids featuring the same dimethylamino head group with different tails and introduced an ester linker into the hydrophobic chain. The existence of an alkyne group in the tail significantly improved the fusion speed and fusion efficiency with endosomal membrane lipids at low pH, further promoted cargo release, and even showed a superior *in vivo* mRNA delivery efficiency than the alkene structure. Meanwhile, to function as a biodegradable segment within the lipid tail, the ester bond reduced the inflammation response of LNPs, leading to lower toxicity associated with repeat dosing.

Besides the functional groups, branching or multi-tail structures in the hydrophobic tail also significantly impact the properties of lipids. Liu *et al.*[44] systematically investigated the effect of tail symmetry and the number of tails on the delivery efficiency of LNPs (Fig. 3A). The symmetry of the carbon chain length or unsaturation degree of the tail structure exhibited the potential to improve the *in vivo* performance of the LNPs. Interestingly, the lipids with 4 tails exhibited a much stronger delivery efficiency than the structures with fewer hydrophobic tails. An increase in lipid tail number led to an augmented cross-sectional area and accelerated the formation of an inverse hexagonal phase for mRNA escape. On the other hand, Hajj *et al.*[45] proposed that a small difference in the branched structure of the lipid tail remarkably enhanced the therapeutic efficacy of mRNA. The one-carbon branch at the terminals of hydrophobic tails exhibited stronger ionization at the endosomal pH of 5.0, refining the delivery efficacy by 10 times compared with their straight-tail counterparts. The branched structure increased the distance between the molecules in the lipid bilayer to form additional space, which reduced the repulsion between the adjacent cations to promote protonation. The study of Yan *et al.*[46] also further demonstrated that branched tail structures in lipids adjusted the hydrophobic domain with moderate hydrophobicity and stability (Fig. 3B). In contrast to the excessively tight assembly of LNPs resulting from a straight tail, the branched structure allowed more efficient mRNA release from LNPs and further strengthened their delivery performance. Therefore, it can be primarily concluded that the tail structures mainly affect the properties of LNPs by regulating their hydrophobicity, membrane fusion efficiency, and inverse HII formation based on lipid shape. These basic characteristics may also further contribute to the modulation of the targeting ability of LNPs. For example, Hashiba *et al.*[47] reported a potential mechanism between LNP spleen tropism and lipid tail length. Interestingly, lipids with shorter tails reduced their molecular volume and further changed the volume contribution of each component, which strengthened the surface density of the rigid phospholipids in the LNP formulation. Augmented rigidity decreased membrane fusion and led to less ApoE adherent on the LNP surface, redirecting liver targeting to spleen targeting. Thus, when considering the modulation of lipid-targeting capacity through tail structures, the influence of different factors could be more complex than expected. This indicates that a clearer understanding of structure–activity relationship is required, particularly regarding the interactions that may arise between different influencing factors.

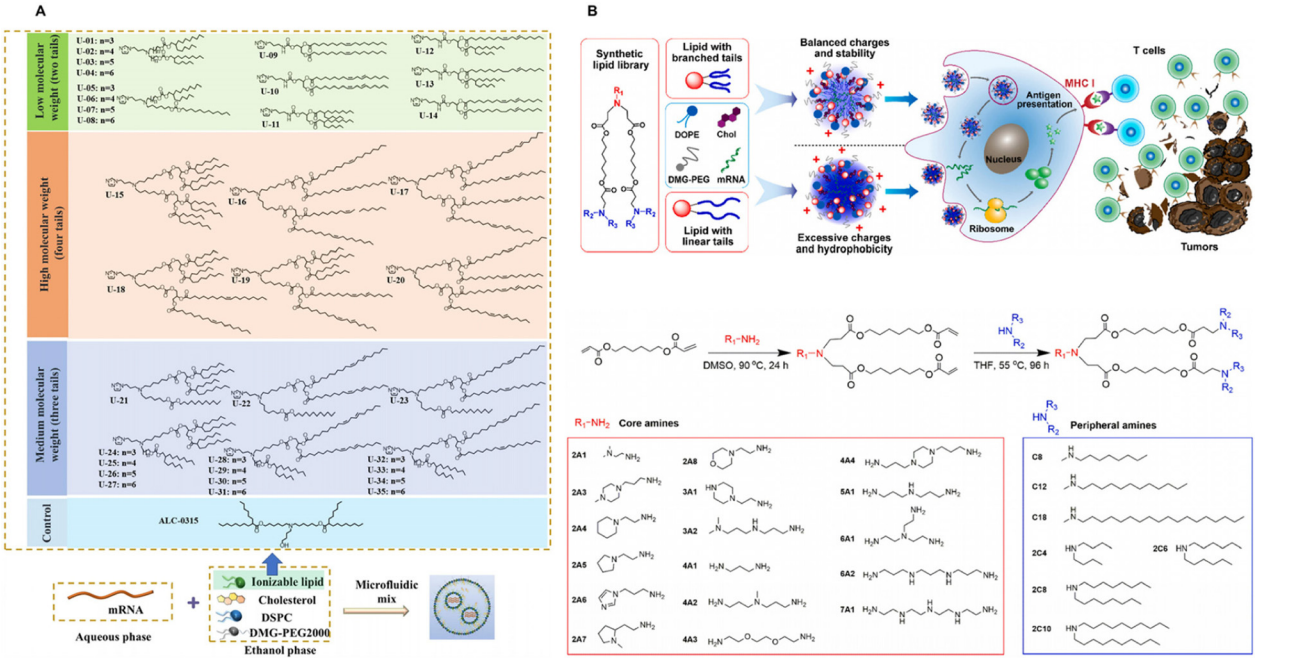

Fig. 3 (A) Structures of ionizable lipids with different numbers of tails and the preparation of LNPs. Reprinted with permission from ref. 44. Copyright 2024, Elsevier B.V. (B) Synthesis of combinational lipids with branched or non-branched tail structures for cancer immunotherapy. Reprinted with permission from ref. 46. Copyright 2023, Elsevier B.V.

2.2 Polymer

Lipids have been well-developed as mRNA vector materials with high transfection ability and safety to lead advancements in the clinical translation of mRNA therapy, but their application is still limited by storage issues due to their suboptimal thermostability, which requires expensive cold chains and logistics.[48] Commonly, lipids exhibit relatively low phase transition temperatures, causing them to remain viscous liquids even at low temperatures, resulting in thermosensitivity.[49] Therefore, other lipid-like structures, such as lipid-like polymers, have been proposed as alternatives to lipids for mRNA delivery. Polymer-based mRNA carriers display superior long-term storage stability. Also, the structure of polymers can be more precisely controlled with excellent batch-to-batch reproducibility.[18] At present, polymer materials utilized as mRNA carriers can be generally divided into poly(ethyleneimine) (PEI),[50] poly(amino acid)s,[51] poly(L-lysine) (PLL),[52] and poly (amidoamine) (PAMAM) dendrimers.[53] The key elements of polymer structures are very similar to those of lipids, also relying on a cationic amine group to efficiently interact with mRNA, and the polymer-related structure–function relationship can be largely inferred from lipid structures. However, compared with small-molecule lipids, polymer molecules exhibit larger molecule sizes and more complicated structures, resulting in severe steric hindrance between neighboring cationic groups. Therefore, lipid-like polymers usually require a higher N/P ratio to be fully complexed with mRNA due to the presence of numerous unpaired cationic groups within the polymer structure.[54] This example highlights the structural disparities between polymers and lipids when utilized as mRNA delivery vectors. The most prominent structural difference between polymers and lipids lies in the long and repeated backbone chain that supports polymer formation and unit arrangement. The chemical structure and physical properties of the polymer backbone will further affect the function and stability of mRNA-loaded polyplexes. Miyazaki *et al.*[55] revealed the influence of block polymer rigidity on the transfection efficiency and stability of mRNA. They first synthesized different cationic block polymers with varying flexibility, including the relatively more flexible PEG-poly(glycidyl butylamine) (PEG-PGBA) based on a polyether backbone, and relatively more rigid PEG-poly(L-Lysine) (PEG-PLL) based on a peptide backbone. The enhanced flexibility of PEG-PGBA was attributed to the lower rotational barrier of C–O–C bonds in the polyether structure. It was found that a flexible polyether backbone permitted a larger contact area and higher binding affinity with mRNA, further amplifying its stability against *in vivo* polyanion exchange and nuclease attack. The enhanced flexibility of the polymer backbone allowed the polyplex to endure the harsh *in vivo* environment with a better transfection performance (Fig. 4A). On the other hand, Li *et al.*[56] concentrated on the variation of the space between side chains located in the polymer backbone and its influence on the *in vivo* performance of polymeric carriers (Fig. 4B). By increasing the distance between the side chain distribution in the polymer backbone, the optimized polymer structure bAC-CART significantly refined the transfection efficacy. The altered side

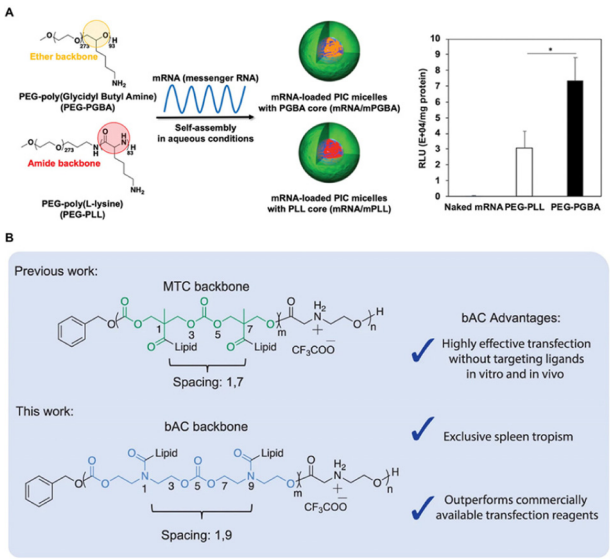

Fig. 4 (A) Preparation of mRNA/m after complexation with PEG-PGBA (mRNA/mPGBA) or PEG-PLL (mRNA/mPLL) and the corresponding bioluminescence in mouse lungs after pulmonary administration of micelles loading GLuc mRNA. Reprinted with permission from ref. 55. Copyright 2020, Wiley-VCH. (B) bAC CARTs possessing a polymeric backbone with a distinct lipid spacing, leading to improved T-cell delivery. Reprinted with permission from ref. 56. Copyright 2023, Springer Nature.

chain spacing also facilitated the charge conversion capacity of bAC-CART and accelerated its intracellular cargo release (Table 1).

Besides the mechanical properties of the backbone, the functional group chemistry in polymers was validated to exhibit a similar performance to that of lipids. For instance, the application of an ethanolamine group as a cationic domain[57] and a branched tail structure as a side chain[58] in the construction of a polymer were both verified to positively affect mRNA delivery. Additionally, a notable advantage of polymeric mRNA vectors is that particle assembly with mRNA can be easily achieved based on one component, which is also a research trend for novel lipid development. The commonly designed LNP systems are composed of 4 different components, which requires cumbersome preparation[59] and suffers from adjuvant side effects such as inflammation and efficacy loss due to anti-PEG antibodies. The proper design of polymer structures can help build stable one-component delivery systems and also regulate their targeting ability *via* small alterations in their functional groups. Zhang *et al.*[60] fabricated a one-component ionizable amphiphilic Janus dendrimer (IAID)-based library. The ionizable amine group in the dendrimers had capacities of dual-hydrophilicity and mRNA binding to allow one-component carrier formation. Meanwhile, changing the linker group from ester to amide converted the liver/spleen targeting to lung tropism. Also, the primary structure of the hydrophobic fragment in IAID obviously contributed to the targeting ability of the dendrimer system, such as differences

Table 1 Summary of the key structure–function relationships of lipid and lipid-like molecules

Molecule category	Structural component	Key structural element	Mechanism and effect	Ref.
Lipid/lipid analogs	Head group	Head group size	Lipid with a smaller head enabled tight packing and generated a more disordered phase in the endosomal environment, enhancing mRNA endosomal escape	28
		Hydrogen bond-forming structure	Hydroxyl bond provided by ethanolamine group enabled the formation of hydrogen bonds with mRNA for better *in vivo* expression than typical lipid DLin-MC3-DMA	31
			Squaramide and thiourea groups increased the hydrogen-bond donor capabilities and favorable π-stacking interactions for enhanced control of the LNP size and stability	32
		Heterocyclic structure	Heterocyclic structure induced a stronger increase in pro-inflammatory cytokines and the related immune response	33
			Heterocyclic lipids displayed excellent transfection and immunostimulatory activities	34
			Cyclic structures could activate STING pathway for the immune response and enhancement in antitumor efficacy of the mRNA vaccine	35
		Siloxane moiety	Siloxane moiety in amine head enhanced the LNP intracellular uptake	36
	Hydrophobic tail	Unsaturated group	Alkyne group in the tail significantly improved the fusion speed and efficiency with endosomal membrane lipids at low pH	43
		Multi-tail structure	An increase in the number of tails in the lipid led to an augmented cross-sectional area and accelerated the formation of an inverse hexagonal phase for mRNA escape	44
		Branching structure	The branch at the terminals of hydrophobic tails underwent stronger ionization at the endosomal pH of 5.0, refining the delivery efficacy by 10 times	45
Polymer	Backbone	Backbone rigidity	Flexible polyether backbones permitted a larger contact area and higher binding affinity with mRNA and better systematic stability	55
		Space between side chains	Increased side-chain spacing facilitated the charge conversion capacity and accelerated intracellular mRNA release	56

in the alkyl group length, nonsymmetric branches and parity of carbon atoms. Conclusively, based on the analogous structure–activity relationship of lipids, the design of polymeric mRNA vectors could be more clearly modulated. However, more attention should be given to the structural arrangement of the polymer backbone, which is the distinctive property of polymers and sometimes reveals complex structure–function mechanisms.

3 Structure-targeting relationship of lipid and lipid-like molecules

The effectiveness of mRNA therapy relies on sufficient mRNA accumulation at the target sites, which remarkably enhances the therapeutic efficacy, minimizes the administered dose, and further reduces the risk of systemic toxicity and associated adverse effects. However, due to the natural liver tropism of traditional LNP-based mRNA carriers, it still remains a challenge to precisely deliver mRNA to specific cells and organs with different physiological structures and microenvironments.[61] To equip carriers with precise targeting capacity, a deeper understanding of the structure-targeting relationship is needed, particularly regarding organ-specific structural features. Advanced mRNA targeting strategies for organ-specific delivery based on lipid and lipid-like polymer structures are discussed in this section, including ligand-mediated and ligand-free organ-targeting structures, commonly utilized selective organ targeting (SORT) adjuvant component structures, as well as structures responsive to some specific intracellular microenvironments.

3.1 Lung-targeting structures

As a critical therapeutic target in the disease, the lungs have been mainly treated with mRNA agents *via* intratracheal delivery.[62] Nevertheless, their delivery efficacy is relatively limited by some biological barriers such as the mucus layer on the surface of the tracheas and bronchi.[61,63] To enhance the mRNA delivery efficiency to the lungs, regulation of lung-targeting ability based on specific chemical structures is expected to improve the therapeutic efficacy of mRNA through both inhalable delivery and systemic delivery.

3.1.1 Ligand-free structures . Recently, it was reported that structures with strong electropositivity could reshape the lung-targeting ability of mRNA carriers, such as quaternary ammonium groups. Huang *et al.*[64] reconstructed a novel lipid-like compound with excellent spleen tropism they developed before[65] by the quaternization of its secondary amine with stronger cationic charges. The quaternization of the ionizable section in the lipid-like molecule significantly changed the profile of its interacted protein corona and exhibited ultra-high delivery selectivity to the lungs, allowing mRNA to be predominantly internalized by pulmonary immune cells. Charge modulation of the head group structure revealed great potential as a ligand-free targeting strategy for lung delivery. Meanwhile, Zeng *et al.*[66] also validated the lung tropism resulting from quaternization by developing a derived quaternary ammonium lipid counterpart of a liver-targeted ionizable lipid (Fig. 6A). The quaternization of the tertiary amine head group in the lipids with high-performing liver-targeting capacity significantly facilitated the liver-to-lung tropism of the LNPs. Furthermore, they performed the same quaternization to reconstruct the clinically applied lipids SM-102 and ALC-0315 to prove the universality of this lung-targeting strategy to different chemical structures, and the delivered mRNA mainly transfected pulmonary endothelial and epithelial cells in this approach. Building on these studies, it can be preliminarily concluded that the highly enhanced cationic property of LNP serves as a broadly applicable approach to promote mRNA accumulation and protein expression in the lungs.[67] This phenomenon can be attributed to alterations in the surface protein corona composition induced by charge changes in the LNPs. The main components in the protein corona of the conventional lung-targeting LNP systems are serum albumin, fibrinogen beta chain, and fibrinogen gamma chain.[61] One hypothesis suggests that highly positively charged LNPs demonstrate greater affinity to interact with serum albumin, which directs the particles to accumulate in the first capillary bed on their journey to the lungs *via* systemic administration.[68] A similar mechanism was also mentioned in the study by Huang *et al.*,[64] revealing that the conversion of tropism from spleen to lung may result from a change in surface absorbed hemoglobin subunit alpha to fibrinogen gamma chain, fibrinogen beta chain, and vitronectin.

Therefore, other structures can directly affect the protein corona profile of LNPs, emerging as a potent strategy to achieve lung targeting. Qiu *et al.*[69] designed a library of amide bond-containing lipidoids (N-series LNPs). By simply changing the ester bond linkage in the original lipid structure to an amide bond, the N-series LNPs could almost exclusively deliver mRNA to the lungs after systemic administration rather than their original liver tropism. The amide-containing tail structure was hypothesized to present specific affinity with serum protein to enhance their lung accumulation. Moreover, the targeting of different pulmonary cells could be easily modulated by slightly altering the amine number and structure in the head group to produce a delivery preference to pulmonary immune cells. Another popular structure usually applied in lung delivery structures is poly(β-amino esters) (PBAE), a polymer with repeating amino–ester bonds in its backbone, which has been considered a safe and biodegradable polymer material for mRNA delivery with good monomer availability and characteristic facile synthesis.[70] Le *et al.*[71] optimized PBAE nanoparticles to achieve selective lung transfection of bevacizumab-encoding mRNA for tumor angiogenesis inhibition (Fig. 5B). Notably, while performing proteomic analysis of PBAE NPs with strong lung tropism, the researchers did not observe adherent apolipoprotein E and albumin, which are usually enriched on the NP surface, leading to liver accumulation. This protein corona profile potentially explained the lower liver transfection efficiency and pulmonary endothelial cell selectivity of PBAE NPs. Similarly, Kavanagh *et al.*[72]

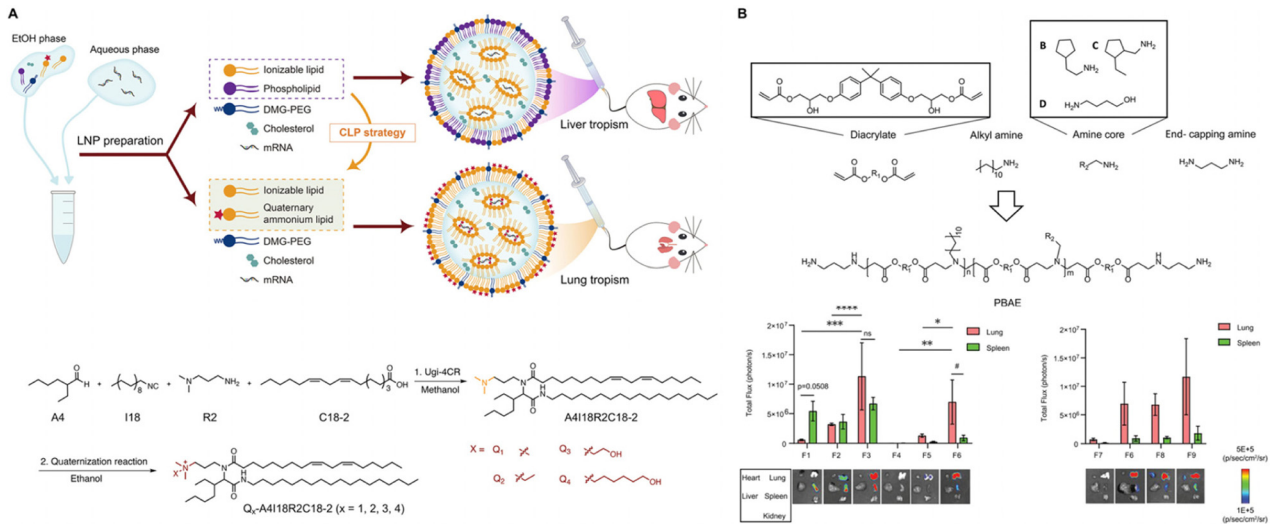

Fig. 5 (A) Schematic of LNP tropism conversion from the liver to lungs by the CLP design strategy with the quaternization and synthesis route of the corresponding quaternary ammonium lipid structures. Reprinted with permission from ref. 66. Copyright 2024, ACS. (B) Library of the PBAE polymers for lung-targeted mRNA delivery and *ex vivo* bioluminescence of the major organs of BALB/c mice that received a Fluc mRNA-loaded polyplex with different formulations. Reprinted with permission from ref. 71. Copyright 2024, ACS.

created a novel PBAE-based polymer that could efficiently transfect pulmonary epithelial and alveolar cells. In their previous study, it was identified that the increased hydrophobicity and specific endcap groups of PBAEs could drive the carrier specifically to endothelial cells following systemic administration.[73] They developed a new hyperbranched cationic PBAE with a hydrophilic heterocyclic and lipophilic alkyl side chain, PBAE-E63, promoting *in vivo* mRNA delivery to the lungs. The lung-targeting capability was speculated to originate from one or more serum proteins in the PBAE-E63 protein corona, while excluding the involvement of lung-specific ligands. This ligand-free targeting strategy not only minimizes the potential immunogenicity to protein ligands but also further simplifies the scaled-up production of materials. On the other hand, the thiol group in the PBAE structure exhibits a unique function in promoting the lung delivery of mRNA. Based on the fundamental structure of PBAE, Rotolo *et al.*[62] fabricated a set of 166 polymers with a diacrylate backbone and amino thiol components for the inhalable administration of mRNA. Compared with formulations lacking the thiol component, the thiol-modified polymer led to increased protein expression, and this trend could be validated in both small and large species. It is also worth noting that the participation of the thiol group refined the codelivery efficiency of long mRNA and short CRISPR RNA in the same system, revealing great potential for synergy with CRISPR-based therapeutics.

3.1.2 Ligand-mediated structures. Ligand-based LNP designs for active targeting are less commonly employed for mRNA delivery to the lungs compared with the strategies of adjusting the LNP structures and components. Although lung-related ligands have still not been fully investigated, some studies still contribute to developing ligand-mediated lung-targeting LNP systems. For instance, Parhiz *et al.*[74] conjugated mRNA-LNP with PECAM-1, an antibody specific to vascular cell adhesion molecules, to dramatically improve the lung delivery efficiency, mRNA transfection and protein expression in the lungs. The participation of antibodies obviously inhibited the hepatic uptake and further enhanced mRNA transfection and protein expression by 25-fold. To explore more ligands that can target the lungs, Soto *et al.*[75] developed a novel peptide to overcome mucus/cellular barriers and enhance the specific mRNA delivery to airway epithelia. They screened and identified mucus-penetrating peptides through T7 phage display and incorporated the screened peptide C into LNPs to achieve distinct selective mRNA transfection in airway epithelia. The exploration and application of cell-penetrating peptides could be a possible trend to facilitate ligand-mediated lung-targeted delivery, especially to overcome the mucus barrier in airway gene therapy.[76]

3.2 Immune organ/cell-targeting structure

As optimal delivery sites of mRNA-based vaccines, lymphoid organs such as the spleen and the lymph nodes contain diverse immune cell populations including T cells, dendritic cells (DCs), macrophages, and B cells,[77] which can effectively initiate strong immune responses and facilitate therapeutic efficacy.[78] Current approaches for delivery to lymphoid organs predominantly rely on intramuscular or subcutaneous administration. Nevertheless, the humoral immunity induced by intramuscular injection is limited by the small amount of transfected dendritic cells in skeletal muscle.[79,80] Compared with local administration, intravenous injection has been reported to generate a more robust antigen-specific CD8+ T cell response for mRNA-based cancer vaccines.[81,82] However, the original liver tropism of mRNA vaccines may lead to reversible hepatic damage, and some mRNA reagents could even be intracellularly reverse-transcribed as DNA in the human

hepatic cell line and produce potential adverse effects.[83] Accurate modulation of targeted delivery to lymphoid organs *via* systemic administration still remains significantly challenging in mRNA-based therapy, requiring further optimization of carrier structures.

3.2.1 Ligand-free structures. Similar to the lung-targeting strategy, precise delivery of mRNA to lymphoid organs can also be achieved by the adjustment of electrical properties, while preferential accumulation in lymphoid organs is supported by the modification of negatively charged structures,[67] such as phospholipids. Liu *et al.*[84] reported the synthesis of zwitterionic phospholipidated polymers (ZPPs) based on the post-modification of alkylated dioxaphospholane oxides for specific mRNA delivery to the spleen and lymph nodes (Fig. 6A). The introduction of a negative phosphate group endowed the polymer with inherent splenic cell transfection capacity, which resulted in a reduction in the surface charge and pK_a of the nanoparticles and substantially amplified the spleen-selective protein expression efficacy compared with the non-phospholipidated cationic polymer. The optimal ZPP structure also enabled the efficient delivery of mRNA to iliac, axillary, and mesenteric lymph nodes. This modular modification of phosphate could be potentially developed as a generalizable strategy for targeting immunotherapeutic applications. Similarly, Zhao *et al.*[85] synthesized poly(L-glutamic acid)-based phosphatidyl polymeric carriers (PLG-PPs) with spleen tropism. They modified the side chain of poly(L-glutamic acid) with phospholipids through a combination reaction with alkylated dioxaphospholane oxide molecules (PLs) to construct a phosphatidyl polymer library with diverse phospholipid tails and phosphate amine groups. Notably, the incorporation of phospholipid transformed the polymers initially lacking transfection efficiency into effective mRNA delivery platforms. The existence of phospholipid tails led to a significantly augmented protein expression in the spleen, which constituted 69.73% of that in the major organs. Additionally, the length of the hydrophobic phospholipid tails was speculated to be part of the possible targeting mechanism to affect the cell membrane penetration by the nanoparticles and direct them to be taken up by specific immune cells. This implies that the function of phospholipid structures in lymphoid organ targeting is far more than simple surface charge regulation. Phospholipid participation in carrier structures was also found to improve the membrane fusion, cellular uptake, and endosomal escape performance of nanoparticles.[84,85] Meanwhile, the reduction in positive surface charge induced by the phospholipid mediated an increase in the serum stability and biosafety of an mRNA carrier for favorable therapeutic efficacy.[84]

Heterocyclic structures, which are highly relevant to the immunogenicity of LNPs, as discussed above, interestingly

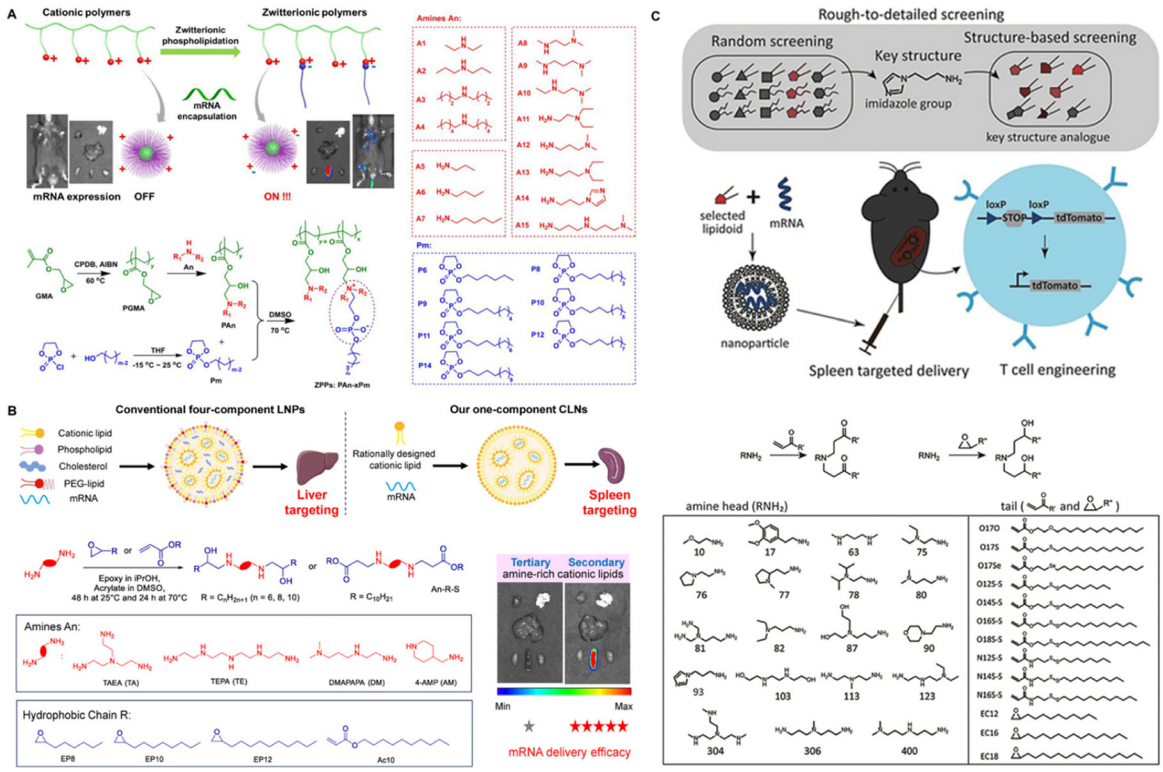

Fig. 6 (A) Combinatorial library of ZPPs synthesized by the phospholipidation of cationic polymers for *in vivo* mRNA delivery. Reprinted with permission from ref. 84. Copyright 2021, ACS. (B) Rational design of one-component ionizable cationic lipids for mRNA delivery to the spleen, with a comparison of the tertiary amine and secondary amine function in spleen targeting. Reprinted with permission from ref. 88. Copyright 2024, Wiley-VCH. (C) Schematic of rough-to-detailed screening of the imidazole-containing lipidoids for spleen/T cell targeting and related chemical structures used for lipidoid synthesis. Reprinted with permission from ref. 86. Copyright 2020, Wiley-VCH.

present potential immune-related delivery selectivity. Zhao *et al.*[86] fabricated an imidazole-containing lipidoid library, which was beneficial to specifically deliver mRNA to T lymphocytes (Fig. 6C). The mRNA transfection to primary T lymphocytes based on non-viral vectors showed limited efficiency, even using the commonly used commercial Lipofectamine 2000. Here, the researchers rationalized the imidazole group as the critical structure for enhanced primary T lymphocyte delivery based on their prior blind screening of large amounts of lipidoids with distinct structures. Then, structure differences in the amine head and hydrophobic tail were further studied to identify the lipid with the best performance. The Fluc mRNA-loaded imidazole lipid was demonstrated to display more specific and stronger luminescence expression in the spleen than in the liver. However, apart from T lymphocytes, mRNA transfection could also be observed in B cells, macrophages, and dendritic cells, indicating a possible improvement was needed to enhance the delivery specificity to cell types. In another study, Ni *et al.*[87] screened piperazine-containing lipids to specifically deliver mRNA to immune cells based on high-throughput DNA barcoding. The top piperazine-structured lipid was loaded with Cre mRNA and its expression was obviously observed in Kupffer cells, and macrophages and dendritic cells in the spleen, revealing a strong delivery preference to the immune system.

Additionally, it is worth noting that some minor structure alterations in the key components also contribute to improving the selectivity for lymphoid tissue. Zhang *et al.*[88] highlighted the critical role of secondary amines in lipid structures, demonstrating their effectiveness in promoting selective targeting to the spleen and T cells (Fig. 6B). Rather than the usual four-component LNPs, a series of single-component ionizable cationic lipids abundant in secondary amines was developed in this research, which presented four-orders of magnitude higher mRNA transfection efficiency than their tertiary amine lipid counterparts. The common liver tropism of LNPs was also converted by secondary amine, and the optimal lipid mediated several orders of magnitude higher protein expression in the spleen than in other organs. Multiple amine-derived lipids exhibited a superior performance in transfection and spleen tropism than those with fewer amine groups, revealing the significant function derived from the secondary amine group. It was also noteworthy that the mRNA accumulation in the spleen did not inevitably direct the enhancement of spleen mRNA transfection. This result reveals that spleen targeting depends on not only the mRNA delivery efficiency to specific sites but also on the transfection capacity to specific cell types. On the other hand, Ben-Akiva *et al.*[89] identified the impact of lipid subunit and endcap modification in polymer structures for preferential delivery to dendritic cells. The researchers synthesized a polymeric platform based on PBAE with lipophilic side chains as subunits and different amine groups as end-capping structures, and a disulfide bond was introduced into the backbone for responsive degradation to a reducing environment. The end-capping groups in the polymers containing a secondary amine exhibited stronger transfection in DC 2.4 and BMDC than those containing a tertiary amine, and the efficacy was further improved by the most lipophilic sidechain. Enhanced hydrophobicity resulting from lipophilic subunits also facilitates the uptake of nanoparticles by dendritic cells and stronger endosomal escape, which further supported selective transfection in the spleen. Encouragingly, the optimal polymer structure especially promoted mRNA transfection in dendritic cells in the spleen rather than other antigen-presenting cells such as macrophages and monocytes, revealing excellent selectivity to a particular immune cell subset with a robust immune effect, as dendritic cells are known to be more powerful in initiating an immune response.

Meanwhile, tail structures are usually considered as one of the important factors to control the lymphoid organ tropism of LNPs. Ren *et al.*[90] constructed a lipid library with diverse tail lengths, branching, and saturation. Based on the *in vitro* and *in vivo* transfection performances, they determined that the branched tail structure exhibited a more favorable delivery preference to the spleen than other linear configurations, with a subcellular distribution mainly in macrophages and dendritic cells. Another study by Vrieze *et al.*[91] explored the synthesis of lipid-PEG amphiphiles incorporating cholesteryl or dialkyl lipid structures with varying lengths, which have been identified as effective binders to albumin and play a critical role in facilitating lymphatic transport.[92,93] After achieving the appropriate balance of water solubility, the stronger hydrophobicity of the lipidic part tended to mediate higher cell uptake level in DC2.4. The lipid-PEG amphiphiles with longer alkyl chains such as didodecyl and dioctadecyl presented more significant accumulation within lymph nodes and stronger *in vivo* cellular interactions, which possibly resulted from the higher attachment to the albumin coating for effective lymphatic drainage.

3.2.2 Ligand-mediated structures. The various receptor profiles on immune cell surfaces within lymphoid organs provide natural targets for selective mRNA delivery, making ligand modification in LNPs one of the most commonly adopted strategies in current targeting mRNA vector design. As the antibodies targeting different immune tissues are quite diverse, some universal small-molecular ligand structures for immune organs and cells and their application are mainly discussed here.

Phosphatidylserine (PS), a potent signalling molecule recognized and internalized by macrophages *via* scavenger receptors, is usually utilized to enhance the endocytic activity of macrophages against enveloped viruses.[94,95] Building on this, Luozhong *et al.*[96] incorporated 2-dioleoyl-*sn*-*glycero*-3-phospho-L-serine (DOPS) into a conventional MC3-based lipid nanoparticle formulation with four components. The standard MC3-LNP formulations predominantly direct mRNA-driven protein expression to the liver. In contrast, incorporating PS into LNPs imparted a negative charge and an immune-cell-targeting ligand, effectively shifting the delivery site to the spleen. Compared with another anionic control LNP lacking the functional phosphoserine group, the PS-loading particles exhibited 45-fold stronger transfection efficacy in the spleen.

Interestingly, the PS-loaded LNPs could obviously alter the *in vivo* distribution of mRNA expression with a selectivity higher than 90% to the spleen and superficial cervical lymph nodes at a low dosage, even if most of particles accumulated in the liver. This result reveals that particle distribution may not be a prerequisite for mRNA transfection and protein expression. Instead, these processes are more likely governed by interactions with specific target cells, such as the preferential transfection of PS-LNPs to macrophages. Notably, the spleen-selective protein expression was slightly reduced when the dosage was increased, which was attributed to the stronger protein expression capacity in liver cells. Likewise, Gomi *et al.*[97] designed secondary lymphoid tissues targeting lipid nanoparticles based on phosphatidylserine. The limited solubility of PS in alcohol hindered its application in LNPs *via* microfluidics preparation, and thus the researchers conjugated linoleic acid and a short acyl group to the PS head domain to synthesize a set of alcohol-soluble PS derivatives. Then, the phosphatidylcholine (PC) component in the standard LNP formulation was replaced by the synthesized PS. In contrast with PC-LNP, PS-PNP was internalized efficiently by immune cells derived from lymph nodes and the spleen, such as macrophages, B cells, and T cells. The accumulation and expression of PS-LNP were also 2.6-fold higher than that of PC-LNP, which resulted from the stronger affinity with the macrophage subpopulation in the marginal zone of the spleen.

Carbohydrate-based moieties are also traditional structures utilized to enhance the selectivity for immune cells in mRNA delivery, especially mannose, whose receptors are widely expressed on macrophage surfaces. Chen *et al.*[98] reported the application of diverse carbohydrate ligands such as mannose, galactose, dextran, and a mixture of mannose and galactose in macrophage targeting. Carbohydrate-modified cationic LNPs or polymeric particles exhibited a stronger propensity for endocytosis by macrophages, and the gene transfection efficiency was highly related to the internalization degree of macrophages. The transfection capacity also relied on the type and content of carbohydrates. Mannose and dextran displayed significantly favorable active targeting ability and transfection efficiency than the other ligands. Fan *et al.*[99] developed a glycan-functionalized polymer to target the DC-SIGN receptor on the macrophage surface. The polymers based on the guanidine group were fabricated using initiators with different glycan head structures, which could be recognized by lectin receptors including Siglec-1, Siglec-2, Siglec-5/E, and DC-SIGN located on dendritic cells and the surface of macrophages.[100] The optimal aryl tri-mannoside was identified as the optimal ligand owing to its exceptional uptake by antigen-presenting cells (APC). Additionally, the binding affinities to the mannose receptor and DC-SIGN receptor of the derivatives, such as linear tri-mannose and branched mannose, were also explored in detail. The strong selectivity to APCs was further demonstrated to significantly enhance antibody expression mediated by the mRNA vaccine.

Compared with strategies for enhancing lung targeting, which typically rely on specific groups to increase the positive charge, lipid design for immune organ targeting is more diverse and influenced by multiple factors. This is due to the greater cellular heterogeneity and complex microenvironment in immune organs. Nonetheless, these physiological characteristics provide additional opportunities for designing immune-targeting lipids. The general strategy using negatively charged phospholipid structures is to promote the adsorption of spleen-affinitive proteins (*e.g.*, β2-GPI)[27] and formation of a protein corona that facilitates lymphatic transport and clearance *via* splenic filtration. Beyond simply providing negative phosphate groups, variations in hydrophobic tails can modulate membrane fusion, allowing the uptake by different immune cells to be tailored. Furthermore, the diverse receptor expression within immune tissues offers additional guidance for targeted delivery. Thus, the complex immune microenvironment presents both challenges and opportunities for the rational design of lipid carriers with tunable targeting properties.

3.3 Other organ-targeting structures

3.3.1 Bone-targeting structures. Bone is a type of connective tissue primarily constituted by a combination of collagen proteins and calcium phosphate minerals,[101,102] containing a complicated microenvironment composed of bone cells, hematopoietic stem cells, immune cells, *etc*.[103,104] However, the dense cortical structure, blood–bone marrow barriers, and low blood flow[105] within the bone microenvironment present significant barriers to the effective delivery and utilization of gene drugs. To improve the bone-targeting efficiency, bisphosphonates (BPs), one of the common drugs for osteoporosis treatment,[106] have been explored as possible delivery ligands. BPs possess a strong binding affinity and rapid adsorption to the bone surface due to their capacity to chelate calcium ions (Ca^{2+}) in hydroxyapatite (HA), which is the primary inorganic constituent of bone.[107] Xue *et al.*[108] synthesized a library of BP-modified ionizable lipid-like materials to formulate LNPs with enhanced bone-targeting ability (Fig. 7A). Compared with the non-BP structures, the BP-functionalized LNPs exhibited higher affinity to bone surface and HA, leading to increased accumulation in the bone site. The transfection efficacy of the delivered BMP-2 mRNA was also amplified in a series of cell types in bone marrow including B cells, T cells, monocytes, granulocytes, and endothelial cells, which facilitated the production of bone morphogenetic protein-2 (BMP-2) to help bone regeneration. Analogously, Yoon *et al.*[109] formulated a series of BP-decorated novel ionizable lipids based on a piperazine ring (PIP) and amides, which could tightly conjugate with the BP group. The movement of the BP groups was limited on the surface of LNPs through their robust interaction with the chair-shape structure of PIP to maximize the binding efficiency with bone. Additionally, the amide groups and hydrophobic chains in the BP-PIP lipids promoted endosomal escape to achieve increased mRNA transfection efficacy in bone.

3.3.2 Pancreas-targeting structures. Gene therapy holds significant promise as a therapeutic approach for incurable pancreas-related diseases, including diabetes and pancreatic

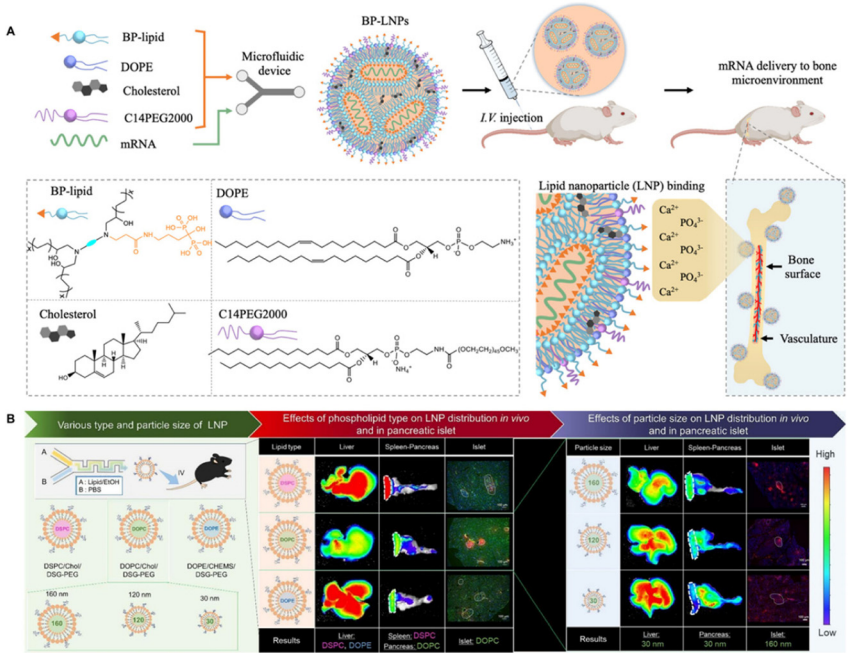

Fig. 7 (A) Schematic of the lipid nanoparticles (LNPs) containing BP lipid-like materials (BP-LNPs) to enable the systemic delivery of mRNA to the bone microenvironment. Reprinted with permission from ref. 108. Copyright 2022, ACS. (B) Schematic of lipid nanoparticles with different sizes and *in vivo* biodistribution in the liver, spleen-pancreas and islet. Reprinted with permission from ref. 111. Copyright 2024, Elsevier B.V.

cancer.[110] However, the non-invasive selective delivery of mRNA based on non-viral vectors to the pancreas still remains challenging currently. Delivery specificity for the pancreas has been pursued through regulation of the physicochemical properties and targeting ligand structures of mRNA carriers. Oguma *et al.*[111] reported that the regulation of LNP sizes and components could affect the LNP distribution in the pancreas (Fig. 7B). By testing different structures of phospholipids in LNPs, it was found that 1,2-dioleoyl-*sn*-glycero-3-phosphocholine (DOPC) exhibited apparently selective biodistribution in the pancreas, deviating from the typical hepatic or splenic accumulation seen with other lipid molecules. The pancreatic distribution was attributed to the distinct structural rigidity and unsaturation of the tail chain. By altering the ratio of components to affect the particle size, the DOPC-based LNPs with a larger size preferred to accumulate in the islets, while smaller LNPs could penetrate the exocrine gland and be further degraded by pancreatic β cells. In another study, Issac *et al.*[112] utilized vitamins as endogenous ligands for targeted mRNA delivery to the pancreas. Notably, cholecalciferol (vitamin D3) was identified as the targeting component within the LNP formulations, achieving an impressive pancreas selectivity exceeding 99% following systemic administration. The cholecalciferol-doped LNPs also displayed pancreas-specific gene editing with excellent biocompatibility, making them well-suited for repeated administration.

3.3.3 Brain-targeting structures. The brain serves as a crucial therapeutic target for various major diseases, including ischemic and hemorrhagic stroke, encephalitis,[113] neurodegenerative disorders, and brain tumors. The contemporary approach in brain-targeted mRNA therapy primarily focuses on the effective penetration of the blood–brain barrier (BBB) *via* systemic administration to enable the selective delivery of therapeutic agents to specific pathological sites in the brain through functionalization of barrier-penetrating ligands. Han *et al.*[114] designed a peptide-functionalized LNP to specifically facilitate the mRNA therapeutic efficacy in the brain. Peptides whose receptors were overexpressed on the brain endothelial cells and neurons, such as RVG29, T7, AP2, and mApoE, were conjugated to LNP *via* click chemistry. The optimal RVG29-containing LNP formulation was found to significantly improve the mRNA transfection efficiency in neurons. Notably, the incorporation of peptides reduced the particle entrapment by the endothelial cells of the BBB. However, the LNP size increased due to peptide conjugation, which might limit the diffusion of the particles into deeper regions of the brain parenchyma. On the other hand, researchers also emphasized the potential of mRNA delivery to restore the integrity of the blood–brain barrier (BBB) after pathological disruption. Gao *et al.*[115] reported the synthesis of a mannose-modified LNP exhibiting high affinity with M2 microglia, which could promote the targeting accumulation of nanoparticles in an ischemic brain and improve poststroke recovery. The size of the IL-10 mRNA-loaded LNP was controlled to around 90 nm, permitting its efficient penetration of the leaky BBB into the brain parenchyma. Then, the LNP was recognized by the CD206 receptor on the M2 microglia mediated by the mannose moiety and targeting expressed IL-10 to facilitate the transformation of microglia toward M2 phenotypes, which presented a positive feedback loop to restore the disrupted BBB.

3.3.4 Ocular tissue-targeting structures. mRNA-based therapy provides significant opportunities for addressing diseases affecting the ocular tissue, owing to the easy accessibility, anatomical separation, immune-privileged, and relatively lower administration dosage[116] of the ocular site. At present, the predominant delivery route of mRNA to the retina is local administration,[117] given that the therapeutic feasibility of systemic delivery has been greatly limited by the blood-ocular barrier. Currently, targeted delivery strategies have emerged as a promising solution to enhance the transfection efficacy, especially through affinitive structures and ligand modification. Eygeris *et al.*[118] designed a series of heterocyclic ionizable lipids (thiol-lipids) based on a thiophene core structure, which demonstrated potent delivery efficiency to the retina. They selected a formulation containing reduced PEG and cholesterol with favorable phospholipids to facilitate subretinal delivery. The thiol-lipid exhibited robust expression in retinal pigment epithelium and photoreceptor with a dosage dependence. Also, adjuvant immune suppression was proved to increase the mRNA expression mediated by thiol-lipid in a combined local and systemic immunosuppressive regimen. On the other hand, Herrera-Barrera *et al.*[119] reported the synthesis of a peptide-conjugated LNP to rapidly localize mRNA into retinal pigment epithelium, and even efficiently cross the neural retina to photoreceptor and Müller glia. The sequence of the conjugated short 7-nucleotide oligomer peptide was screened out by an M13 bacteriophage-based heptameric peptide library. The peptide modification to liver-targeting MC3 lipid effectively mediated successful retinal expression by subretinal injection. Notably, the varying density of peptides on the surface of the LNPs may affect their penetrative properties to interact with specific retinal cell receptors.

3.4 SORT adjuvant component structures

As novel lipid components in LNP formulations, the concept of SORT (selective organ targeting) lipids was proposed by Siegwart in 2020,[120] which are a type of lipid structures utilized to precisely regulate the *in vivo* delivery profile of mRNA through internal charge alteration (Fig. 8A). In our above introduction to the organ-targeting strategy, surface charge modulation moieties in lipid structures play an important role in organ tropism to the lungs and spleen, such as quaternary amine or phosphate groups. In contrast, SORT lipids serve as a fifth component, an independent adjuvant, to regulate the charge of LNPs. By quantificationally controlling their ratio in LNP formulations, SORT lipids enable sensitive alteration in the organ selectivity for mRNA delivery, revealing the potential of helper lipid structures in targeting. In the study by Siegwart, the researchers first chose a permanently cationic quaternary amino lipid, 1,2-dioleoyl-3-trimethylammonium-propane (DOTAP), to systemically increase its percentage from 5% to 100% in the standard 5A2-SC8 LNP based on four typical components. The mRNA expression exhibited a clear delivery conversion from the liver to the spleen with 10%–15% DOTAP, and then to the lung with more than 50% DOTAP. Another SORT lipid, the anionic lipid 1,2-dioleoyl-*sn-glycero*-3-phosphate (18PA), was also demonstrated to drive complete spleen tropism when its percentage reached 10%–40% in a basic four-component LNP, with no mRNA expression in any other organs compared with the original liver affinity. Along with enhanced organ selectivity, SORT LNPs also exhibit significantly improved transfection efficiency of the encapsulated mRNA than normal LNPs. Surprisingly, this functionality of SORT lipids was consistently embodied across different SORT lipid structures with similar charges, as well as in different liposomal formulations, demonstrating the universality of the SORT lipid function. As shown in Siegwart's study, to determine whether tissue tropism of SORT would be limited by exact chemical structures or applicable to various chemical structures with similar charge properties, researchers evaluated multiple permanently cationic and anionic SORT lipids

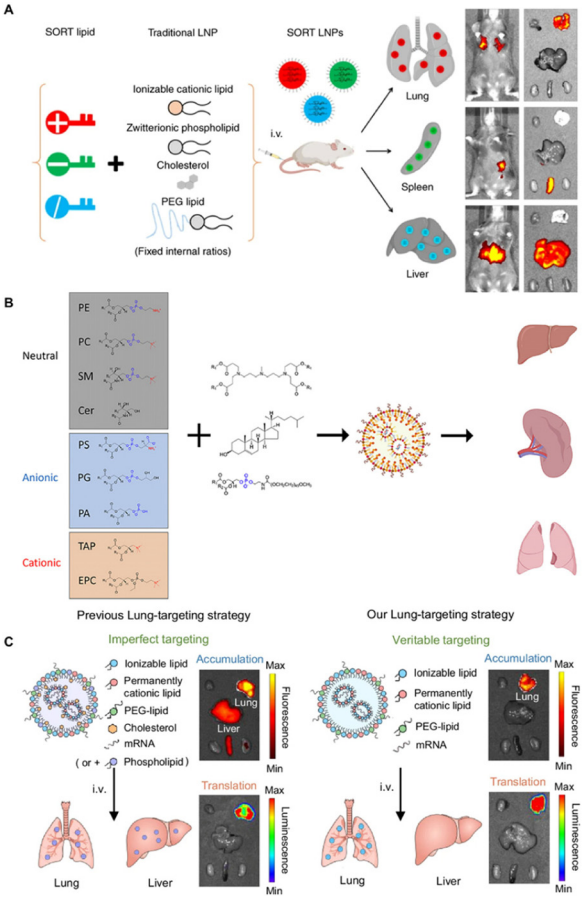

Fig. 8 (A) Addition of a supplemental component (termed a SORT molecule) to traditional LNPs, systematically altering their *in vivo* delivery profile and mediating tissue-specific delivery as a function of the percentage and biophysical property of the SORT molecule. Reprinted with permission from ref. 120. Copyright 2020, Springer Nature. (B) Helper lipid with different charges in lipid nanoparticles leading to different organ tropism in mRNA delivery. Reprinted with permission from ref. 123. Copyright 2022, Elsevier B.V. (C) Schematic of the lung-targeted mRNA accumulation and translation following systemic administration enhanced by removing cholesterol and phospholipid. Reprinted with permission from ref. 124. Copyright 2024, Springer Nature.

with different structures. For instance, two other cationic SORT lipids, dimethyldioctadecylammonium (DDAB) and 1,2-dimyristoyl-*sn-glycero*-3-ethylphosphocholine (EPC), were incorporated in the standard 5A2-SC8 LNP. These two quaternary amine lipids performed the same liver-to-lung target conversion as DOTAP, even with their great chemical differences in the polar headgroup, linker region and hydrophobic domain. Moreover, the properties of same SORT lipids can be generalized to different classes of established four-component LNP systems. Specifically, researchers supplemented the hepatic-tropic standard DLin-MC3-DMA LNPs and the C12-200 lipid-like LNPs with a fifth component, either DOTAP or 18PA. Despite the two standard lipid molecules exhibiting markedly distinct structures in both their head groups and the number of hydrophobic tails, they displayed a similar shift in organ-targeting preference upon the incorporation of the SORT lipid.

To further reveal the detailed mechanism underlying the SORT lipid performance, Siegwart reported another study[27] in 2021 to prove that the specific organ selectivity of SORT was driven by the varying apparent pK_a and surface protein corona profiles of LNPs. It was reported that the protein corona of LNPs could induce the migration of certain lipid components to the surface and rearrange the LNP formulation.[121] By modulating the charged SORT components, the diverse surface chemistries of SORT LNPs might alter the nanodomain to absorb different proteins. It was subsequently discovered that Vtn is a critical protein absorbed by cationic SORT lipids, facilitating binding to highly expressed αvβ3 integrins in the lungs. Meanwhile, anionic SORT lipids demonstrated an affinity to β2-GPI, facilitating their clearance through spleen filtration. The applicability of SORT lipids was expansively proven in other studies, such as that by Luo *et al.*,[122] in which they similarly introduced different anionic SORT lipids, 18PA, DPOG, and DOPS, into an LNP system to enhance dendritic cell uptake.

Building on these findings, the similar function of other adjuvant lipids with more diverse structures was further explored for the targeted delivery of mRNA. LoPresti *et al.*[123] replaced the standard helper lipid component of DOPE with 8 distinct lipid structures including cationic lipids (DOTAP and ethyl phosphatidylcholine), anionic lipids (phosphatidylserine, phosphatidylglycerol, and phosphatidic acid) and neutral lipids (DOPC, sphingomyelin, and ceramide). The delivery trend mediated by the different charged SORT lipids was consistent with previous studies, and it could be systematically concluded that most of the cationic, anionic, and neutral adjuvant lipids led to selective mRNA delivery to the lungs, spleen, and liver, respectively (Fig. 8B). However, according to the difference in lipid structures, the efficiency of targeting mRNA expression also varied, indicating a related mechanism based on the structure–function relationship. An alternative lipid was validated to be competent to play the role of DOPE and could avoid the complexity of a five-component LNP system. Moreover, it was surprising that proper simplification of the lipid components could reduce the off-organ accumulation of LNPs. Su *et al.*[124] reported that the inherent components of cholesterol and phospholipid were dispensable to LNP functionality. The typical design of a four-component formulation unavoidably caused liver tropism through systemic delivery, especially due to the role of cholesterol, which enhanced the lipoprotein coating to interact with liver cells. After removing cholesterol and phospholipid, researchers incorporated the degradable ionizable lipid nAcx-Cm with the SORT lipid DOTAP. The three-component LNPs exhibited superior lung targeting and transfection efficacy than the cholesterol-containing four/five-component LNPs (Fig. 8C). Also, the stability of the LNPs was not affected, and this simplification even presents universality in other existing lipid-based delivery systems.

3.5 Intracellular environment-responsive structures

The introduction of stimuli-responsive structures in LNPs can be an effective approach to promote the specificity of mRNA transfection to target cells or tissues.[125] The microenvironment within organ tissues or cells offers lots of triggers allowing precise mRNA release in the target site, such as abnormal pH value, increased redox potential, and overexpressed intracellular enzymes. Accordingly, functional moieties specifically responsive to these conditions have been widely incorporated within lipid structures to achieve better therapeutic effects. Some novel responsive structures in recent research are introduced in this section.

3.5.1 pH-responsive structures. The local pH value varies in the microenvironment of different organelles, tissue cells and disease sites. Generally, endosomes and lysosomes present a decreased pH range from 6 to 4,[126] and organs (stomach and vagina)[127] and pathological sites (inflammation, infection and tumors) are also characterized as acid environment. To facilitate the selectivity to these acidic tissues and cells, critical pH-sensitive groups have been incorporated into lipid or lipid-like structures, such as orthoesters, imines, maleic acid amides, hydrazone, acetal and cycloacetal bonds.[128–130] Zhao *et al.*[131] developed a set of rapid-degradable lipids containing 'azido-acetal' linker with an excellent delivery performance to various targets, including the liver, lungs, spleen, brain, and haematopoietic stem and progenitor cells. The liver tropism of the typical LNPs stems partly from their more efficient uptake by liver cells, compensating for their low endosomal escape rate.[132] However, targeting non-liver organs demands LNPs with stronger endosomal escape capability. The novel lipid with an azido-acetal linker could undergo hydrolysis at the endosomal pH of 6.0 within a hydrolysis half-life of 14.8 min, while remaining stable at pH 7.4 for 21 days. The strong acid degradation capacity was owing to a two-step mechanism, where the water-stable azido-acetal structure was reduced to an amine through thiol addition and accelerated the next acid-hydrolysis step of the linker. Incorporation of the degradable linker into the structures of PEG lipids, anionic lipids, and cationic lipids notably improved their targeted delivery (Fig. 9A), with PEG lipids showing enhanced expression in the liver and brain, anionic lipids in the spleen, and cationic lipids in the lungs, surpassing the performance

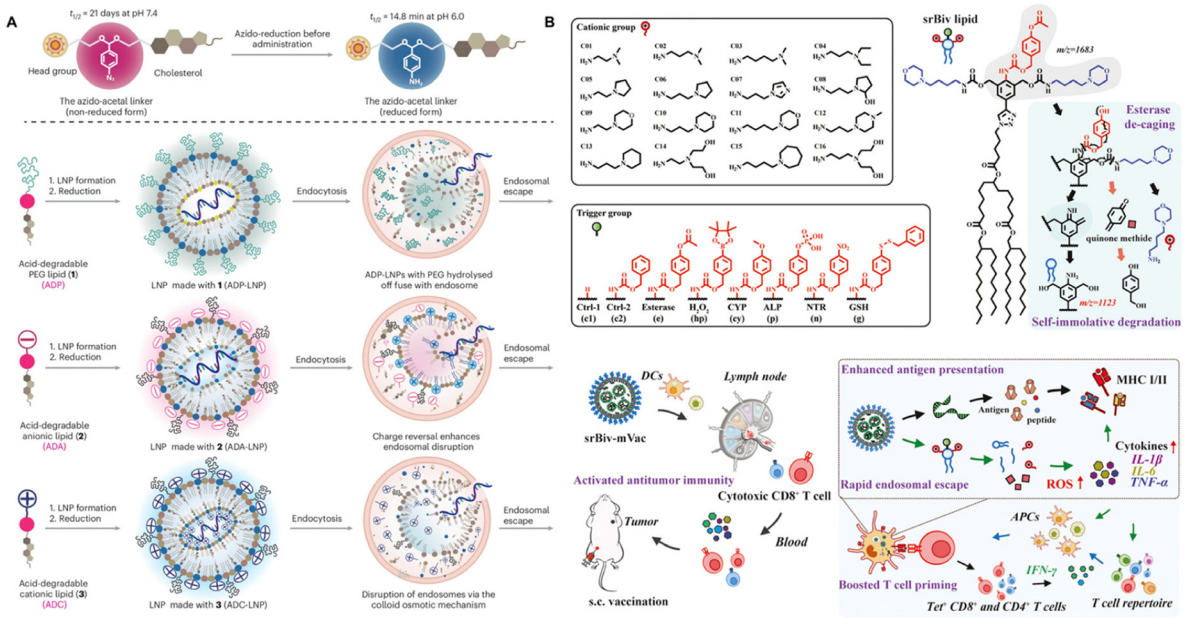

Fig. 9 (A) Acid-degradable linker 'azido-acetal'-containing lipids undergoing rapid hydrolysis in endosomes but remaining stable at pH 7.4, which are applicable in three different acid-degradable lipid nanoparticles (ADLs). Reprinted with permission from ref. 131. Copyright 2024, Springer Nature. (B) Structures of 128 stimuli-responsive bivalent ionizable lipids (srBiv iLPs) and subcutaneous vaccination with eBiv-mVac to induce robust innate and adaptive immune responses. Reprinted with permission from ref. 137. Copyright 2024, ACS.

of their aligned standard lipid. Accelerated release and endosomal escape of mRNA are crucial to amplify the transfection efficiency in the target site. In another study, Cheung *et al.*[133] designed an acid-responsive novel amphiphilic poly(lactic acid)-*block*-poly(carboxybetaine) (PLA-*b*-PCB) zwitterionic polymer. The hemiacetal ester pendant groups in the polymer induced a charge conversion from positive to nearly neutral in response to acidic conditions, and the decreased zeta potential of polymer-containing LNPs reduced their affinity with mRNA to allow more efficient mRNA release in endosomes. Even though the endosomal escape performance mediated by lipids remained at the same level, increased mRNA release from the polymer-doped LNPs apparently strengthened the therapeutic efficacy.

3.5.2 Redox-responsive structures. Pathological conditions disrupt the intracellular redox homeostasis and produces an abnormal redox potential in biological microenvironments, such as the reductive tumor environment with an elevated GSH level three-orders of magnitude higher than the extracellular domain,[134] and oxidizing inflammation environment involving excessive reactive oxygen species (ROS). This notable distinction in redox conditions facilitates effective mRNA accumulation in target cells or tissues. The commonly used redox-stimuli-responsive structures can be divided into GSH-responsive groups (disulfide and diselenide) and ROS-responsive groups (boronates, thioethers, thioketals and sulfides).[121] For example, Chen *et al.*[135] synthesized a series of disulfide-linkage-based ionizable lipids (LDILs) to achieve mRNA-mediated bioluminescence in the precise localization of tumor metastasis. The four disulfide-bond bridge linkers in the optimal molecule 4A3-SCC-10/PH allowed the lipid to form a GSH-responsive cone-shaped architecture, leading to more rapid mRNA release and endosomal escape in tumor cells compared with its parent lipid without a disulfide bond. After intraperitoneal injection, 4A3-SCC-10/PH facilitated faster cell uptake of Fluc mRNA in 4T1 breast cancer cells and B16F10 melanoma cancer cells, presenting the preferential accumulation and expression of luciferase in metastasis. This tumor-responsive bioluminescence strategy can distinguish tumor metastases from normal organ tissues with a high signal-to-noise ratio (SNR). In another study, Wang *et al.*[136] developed an ionizable lipid library containing an ROS-sensitive trisulfide linker to specifically clear the excessive ROS in diabetic wounds and induce the expression of IL-4 mRNA in macrophages. By altering the tail structure, the selected TS2 LNP exhibited superior mRNA transfection 30-fold higher than the clinically used MC3 LNP. The trisulfide linker in the TS2 LNP also enabled an effective response to ROS and protection of fibroblasts against oxidative stress. The stimulated release of IL-4 mRNA in the wound drove the repolarization of macrophages from M1 to M2, promoting the anti-inflammation and healing process of the wound.

3.5.3 Enzyme-responsive structures. Overexpressed enzymes in different cells and tissues can be critical targets for selective mRNA delivery. Enzyme-induced reactions are sensitive, fast, and highly specific based on mild reaction conditions, which efficiently promote localizable and controllable mRNA release in the designated biological site. Currently, structures responding to intracellular esterase and protease (matrix metalloproteinase, cathepsin, *etc.*),[125] such as ester

bonds and peptides, have been frequently utilized to achieve enzyme-stimuli-responsive functions for targeted mRNA delivery. Dong *et al.*[137] fabricated a stimuli-responsive lipid library with different trigger groups for enhanced mRNA vaccine delivery to APC. Various trigger groups responding to esterase, nitroreductase, alkaline phosphatase, and cytochrome P450, *etc*. were introduced into the lipid head domain, and the esterase-responsive lipid (eBiv) was finally screened out as the optimal vector material for APC target delivery (Fig. 9B). The esterase-rich environment of APC facilitated macrophages to rapidly internalize the ester bond-containing LNPs, and prompted the further transportation of the LNPs to draining lymph nodes after subcutaneous administration. Then, abundant mRNA was responsively released to induce a robust immune response of CD8+ T cells for potent antitumor efficacy. Zhang *et al.*[138] also utilized an esterase trigger to design an interesting decationizable quaternium lipidoid, AMB-POC18. The esterase-labile quaternary ammonium group in the lipidoid enabled the conversion of the cationic molecule to an anionic one under esterase-overexpressed conditions. The selected AMB-POC18 molecule possessed an *N*-(*p*-(alkyloyloxy)benzyl) group in each quaternary ammonium moiety, which allowed easier esterase-induced degradation. The preferential hydrolysis of this group transformed quaternary ammonium into a tertiary amine and was further accompanied by hydrolysis of the ethyl ester linkages, which synergistically resulted in a decrease in the zeta potential. This structure achieved a balance between LNP stability and responsive mRNA release to the specific esterase concentration in the spleen, which mediated selective mRNA transfection to APC (Table 2).

4 Biomedical applications

4.1 mRNA vaccines

Vaccines hold pivotal significance in safeguarding public health, which prevent the prevalence of millions of illnesses[139] such as the smallpox virus, hepatitis, polio, and measles. Traditional vaccines function as a potent tool to establish immunological memory against pathogens, significantly lowering the risk of infection upon future exposure.[140] This immunological response is typically achieved by injecting inactivated pathogens or purified proteins. However, the development of conventional vaccines is insufficient to address the rapidly evolving spectrum of pathogens, particularly those capable of evading adaptive immune responses, as well as non-infectious diseases such as cancer. In the context of the COVID-19 pandemic, there is an urgent need for vaccine platforms that can be rapidly developed and adapted for large-scale production, enabling the more effective prevention and treatment of diseases. mRNA vaccines can satisfy the needs of scalable manufacturing and present favorable safety with their non-infectious and non-integrating nature.[141] Moreover, mRNA vaccines allow quick adaption to variants or subtypes of pathogens and provide personalized treatment according to specific antigens from patients.[139,141] For either prophylactic vaccines or therapeutic cancer vaccines, the effect of mRNA vaccines mainly relies on the efficient recognition of mRNA expression by the immune system to stimulate a strong enough immune response. Generally, mRNA vaccines for SARS-CoV-2 deliver synthetic mRNA encoding the viral spike protein and make it expressed, recognized, and taken by antigen-presenting cells for further B cell memory, while cancer vaccines require a more potent T cell response to directly kill antigen-containing tumor cells after the translation of the tumor-associated antigen encoding mRNA (Fig. 10A).[142] mRNA vaccines administered *via* intramuscular injection exert their effect by initiating the recruitment of immune cells through localized inflammatory responses.[143] Nevertheless, most of the mRNA is taken by muscle cells, and part of the residual mRNA is further absorbed by the liver after entering the systemic circulation.[144] To minimize the off-target effect and inflammation side effect, it is crucial to design rational carrier structures that enable efficient targeted delivery of mRNA vaccines to immune tissues *via* systemic administration. As previously discussed, immune-targeting strategies leveraging lipid structural design have demonstrated considerable potential, which promote mRNA drainage to lymph nodes and antigen presentation cells. In a prototypical example, non-ligand modified lipid materials for lymph node targeting could be developed by evaluating the function of different structural sections, especially through the combinational synthesis of diverse amine heads, linkers and tail groups, leading to the sufficient expression of ovalbumin protein and a potent antitumor immune response (Fig. 10B).[145] At present, mRNA vaccines have been widely commercialized and applied in clinical practice. The COVID-19 vaccines developed by Pfizer and Moderna have served as established commercial products, playing an important role in protecting the public health during the pandemic. Meanwhile, over 20 cancer vaccine candidates are currently undergoing clinical trials.[146] It is anticipated that targeted lipid materials will bring new advancements and opportunities to mRNA vaccine-based therapies.

4.2 Protein replacement therapy

Protein replacement therapy has been regarded as a viable solution to replace or supplement specific protein deficiencies caused by mutations in affected patients, which result in protein loss or dysfunction.[147] This technology has been widely utilized as a therapeutic approach for rare diseases,[148] with several related treatments approved by the FDA and entering clinical practice as orphan drugs.[149] In recent years, protein replacement has also exhibited great potential in cancer treatment. Many types of cancers are induced or promoted by the absence or deficiency of certain proteins in specific tissues.[150] For example, in prostate cancer, loss of phosphatase and tensin homolog (PTEN) protein expression stimulates the activation of the PI3K–AKT pathway, which leads to the enhancement of tumor cell survival, proliferation, migration, angiogenesis, and anti-apoptosis.[151] Traditionally, protein replacement is achieved by directly delivering a syn-

Table 2 Summary of the key structure-targeting relationships of lipid and lipid-like molecules

Targeted organ/ environment	Targeting category	Key structural element	Mechanism and effect	Ref.
Lung	Ligand-free	Quaternary ammonium structure	Quaternization changed the profile of its interacting protein corona and exhibited targeting conversion from the spleen to the lungs	64
			Quaternization of the tertiary amine head group significantly facilitated the liver-to-lung tropism of the LNP	65
		Amide bond	Amide-containing tail structure was hypothesized to present the specific affinity with serum proteins to enhance its lung accumulation	69
		Poly(β-amino esters)	Amino–ester structure reduced the adherence of apolipoprotein E and albumin and improved lung tropism	71
		Thiol group	Compared with formulations lacking a thiol component, the thiol-modified polymer led to increased protein expression in lungs	62
		Cationic SORT component	An increase in the DOTAP ratio in the standard four-component LNP exhibited strong lung tropism	120
	Ligand-mediated	Antibody	Conjugation of PECAM-1, an antibody specific to vascular cell adhesion	74
		Cell-penetrating peptides	Mucus-penetrating peptide conjugation achieved distinct selective mRNA transfection in airway epithelia	75
Immune organ/cell	Ligand-free	Phospholipid structure	Introduction of a negative phosphate group endowed the polymer with inherent splenic cell transfection capacity due to reduced surface charge and pK_a	84
			Phospholipid tails led to a significantly augmented protein expression in the spleen, which constituted 69.73% of that in major organs	85
		Heterocyclic structures	Imidazole group as the critical structure for enhanced primary T lymphocyte delivery	86
			Piperazine-structured lipid exhibited obvious expression in Kupffer cells, macrophages and dendritic cells in the spleen	87
		Secondary amines	Secondary amine polymer performed stronger transfection in DC 2.4 and BMDC than those containing a tertiary amine	89
		Branching tails	Branched tail structure exhibited stronger spleen tropism than other linear configurations, with a subcellular distribution mainly in macrophages and dendritic cells	90
		Anionic SORT component	Increase in the 18PA ratio in the standard four-component LNP exhibited strong spleen tropism	120
	Ligand-mediated	Phosphatidylserine	Phosphatidylserine-loaded particles exhibited 45-fold stronger transfection efficacy in the spleen	96
		Carbohydrate-based moieties	Mannose and dextran displayed significantly favorable active targeting ability and transfection efficiency to the spleen than other ligands	98
Bone	Ligand-mediated	Bisphosphonates	Bisphosphonate-functionalized LNP exhibited higher affinity to bone surface and HA, leading to increased accumulation in the bone site	108
Pancreas		Vitamins	Targeting component cholecalciferol (vitamin D3) achieved an impressive pancreas selectivity exceeding 99% following systemic administration	112
Brain		Peptides	Peptides reduced the particle entrapment by the endothelial cells of BBB and improved the mRNA transfection efficiency in neurons	114
Ocular tissue		Peptides	Peptide-conjugated LNP could rapidly localize mRNA into retinal pigment epithelium, and even efficiently across neural retina to photoreceptor and Müller glia	119
pH	Environment-responsive	Azido-acetal/ hemiacetal ester pendant groups	Acid-responsive capacity accelerated the release and endosomal escape of mRNA for enhanced transfection efficiency	131 and 133
Redox		Disulfide bond	GSH-responsive disulfide bond led to more rapid mRNA release and endosomal escape in tumor cells	135
Enzyme		Trisulfide linker	ROS-sensitive trisulfide linker induced the expression of IL-4 mRNA in macrophages by 30-fold than clinical LNP	136
		Ester bond	Esterase-responsive lipid structures enabled excellent antigen-presenting cell target delivery	137 and 138

thetic protein into the disease site, but it is challenging to maintain the stability of proteins within the complex physiological environment and they may present potential immunogenicity.[152] Regarding gene therapy regulating protein expression, the risk of gene integration into the host genome should also be considered. By contrast, mRNA serves as a safer protein replacement agent and almost evades the possibility of nucleus insertion and genetic alteration. Targeted delivery of mRNA to affected tissue allows abundant protein expression in the disease site, which can be effectively achieved by ligand modification in the lipid structure. In a recent study, programmed death ligand 1 (PD-L1) binding peptides were linked to PEGylated lipids through a copper-free click chemistry reaction.[153] The active targeting ability of the PTEN mRNA-loaded

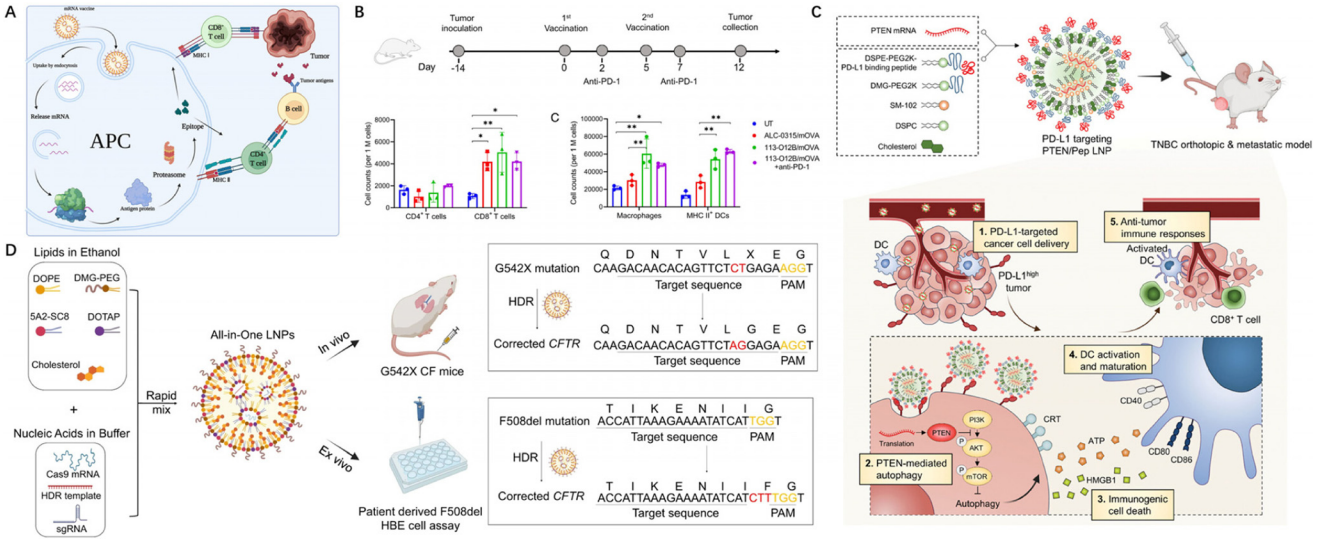

Fig. 10 (A) Schematic of the working mechanism of the mRNA vaccine for cancer therapy. Reproduced from ref. 142. Published by Frontiers Media SA 2022, under the terms of the Creative Commons Attribution License (CC BY). (B) Changes in the immune cell composition in an established B16F10-OVA tumor after vaccination. Reprinted with permission from ref. 145. Copyright 2022, *PNAS*. (C) Schematic of the PD-L1-targeted PTEN/Pep LNP formation and the working mechanism for immunotherapy of TNBC based on protein replacement therapy. Reprinted with permission from ref. 153. Copyright 2024, Wiley-VCH. (D) Schematic of the working mechanism of the SORT LNP-mediated gene correction therapy in CF mouse models based on gene editing. Reprinted with permission from ref. 157. Copyright 2023, Springer Nature.

LNP was mediated by its ligand-induced strong cell uptake in PTEN-deficient triple-negative breast cancer cells (TNBC) (Fig. 10C). The favorable PDL1 binding affinity of the LNPs ensured successful transfection in the targeted tumor cells and further facilitated autophagy-mediated immunogenic cell death through systemic delivery.

4.3 Gene editing

The discovery of the CRISPR/Cas9 system has sparked a revolution in the application of gene editing tools. CRISPR/Cas9 is formed by two essential components: Cas9 enzyme and guide RNA (gRNA). Under the guidance of gRNA, the Cas9 enzyme can recognize the target sequence to form an RNA–DNA hybrid and activate the cleavage of DNA.[154] The double-strand break can be further repaired by the host cellular machinery, which offers opportunities to insert new DNA into original sequence.[155] The delivery of the CRISPR/Cas9 system can be achieved in the form of DNA, mRNA, and ribonucleoprotein (RNP) complexes. Compared with the other two gene editors, the mRNA-based CRISPR/Cas9 system stands out for its faster expression kinetics, genetic safety, and relatively lower immunogenicity. In this approach, CRISPR mRNA and gRNA can be directly introduced into target tissue to express the Cas9 protein and achieve *in vivo* editing of specific genes. Regarding the easy degradation of gRNA during Cas9 mRNA translation, proper chemical modification and sequence optimization have been applied to protect them from hydrolysis,[156] which makes the mRNA-based CRISPR/Cas9 system a promising platform to regulate diverse diseases. To maximize the editing efficacy, CRISPR/Cas9 mRNA should be precisely delivered to disease-related organs or cells. This requirement has been addressed through the use of SORT lipid structures in recent research. For example, an optimized DOTAP LNP was shown to achieve efficient gene correction in a lung cystic fibrosis model harboring the G542X mutation (Fig. 10D).[157] The incorporation of the SORT lipid enabled successful Cas9 transfection to 60% of lung basal cells through systemic administration, demonstrating strong selectivity for the target cells. This strategy overcame the typical liver accumulation of LNPs and also avoided the side effects of traditional viral vectors for gene editor delivery. In another study, lung-targeting SORT LNPs were proved to achieve the effective delivery of CRISPR-Cas9 mRNA into lung stem cells to durably correct mutation and restore function in lung cystic fibrosis.[158] The editing level in the lung cells remained consistent over a 22-month tracking period, illustrating a stable editing effect in the target site.

5 Conclusion and prospects

Targeting mRNA delivery to specific organs or tissues has broadened the therapeutic applications of mRNA, demonstrating significant potential in the treatment of various diseases. Also, the rational design of vector materials based on lipid or lipid-like structures allows more precise regulation of targeting capacity to deliver mRNA. The development of suitable lipid candidates requires large-scale synthesis and screening of a lipid library with numerous combinational structures. Usually, the success rate in selecting a lipid with favorable delivery efficacy *in vitro* is less than 10%.[159] Moreover, the disconnect between the *in vitro* and *in vivo* mRNA delivery performance has become another major hurdle[160] in the development of

novel lipid molecules. A common scenario is that certain lipid structures demonstrating an exceptional transfection performance *in vitro* fail to produce comparable transfection outcomes *in vivo*, and sometimes even exhibit no efficacy due to the complicated *in vivo* environment and possible interaction between LNPs and biological molecules in the systemic circulation and the target site. To simplify the process of lipid library construction, machine learning has been employed to predict the performance of diverse lipid structures,[161] while barcoded DNA/RNA technology has expedited high-throughput screening.[160,162] However, although these advanced technologies have greatly improved the screening efficiency of lipid structures, the detailed structure–function relationship behind the mRNA delivery efficacy of different lipid structures still remains partially unknown. Discovering the universality of special structures in lipid or lipid-like molecules may allow more accurate prediction and modulation of the *in vivo* mRNA delivery efficiency based on related vectors. Some structural characteristics have been found in recent studies to generate a similar effect on the LNP performance across lipids, lipid analogs, and lipid-like polymers, with their role in modulating targeting capability being equally applicable. Therefore, specific head groups, tail chains, backbones, and organ-selective structures have been introduced in this review to reveal possible common patterns in the correlation between lipid or lipid-like structures and mRNA delivery efficiency. By summarizing these universal key structures, some general mechanisms for regulating lipid functions have also been identified, particularly the critical role of surface charge and protein corona components in LNP targeting capability.[27] However, to achieve ideal mRNA expression in the target site, merely enhancing the accumulation of the mRNA vectors in the target organ is insufficient. As in some cases, the biodistribution of the vector particles does not exhibit a positive correlation with their mRNA transfection efficiency. After effectively hitting the target site, more attention should be paid to the lipid properties of enhancing cell uptake, endosomal escape, and transfection affinity in organs. This further requires more precise delivery selectivity not only to targeted organs but to specific cell types, which represents cell microenvironment targeting as a key trend in ongoing innovative mRNA-targeted delivery studies. Meanwhile, a clear understanding of the structure–activity relationship facilitates the simplification of lipid-related structures and lipid nanoparticle components. One current research emphasis is advancing the design of single-component lipid nanoparticles and ligand-free-targeted carriers through rational structural optimization. These efforts aim to streamline industrial production for the more convenient clinical application of mRNA delivery systems in treating non-liver diseases. However, with the increasing understanding of structure–activity relationships and the guidance of structure–targeting correlations, structural optimization of lipids cannot focus merely on performance enhancement. Instead, it is crucial to balance delivery efficiency with potential *in vivo* toxicity arising from specific structural features. Immunogenicity represents a major manifestation of lipid-associated toxicity *in vivo*.[22] Certain structural motifs, such as heterocycles, can enhance immunogenic responses during lipid metabolism. Moderate immunogenicity may provide an opportunity to activate immune cells and enhance therapeutic outcomes, whereas excessive immunogenicity can trigger harmful inflammatory reactions. Another key source of lipid toxicity arises from the off-target effects of mRNA delivery, leading to tissue-specific damage.[163] This underscores the importance of exploring structure–targeting relationships for mRNA lipid nanoparticles, particularly under conditions of repeated or long-term administration. Although further exploration is required to systematically summarize the structure–function relationships and delivery mechanisms of targeting carriers, we remain optimistic that progress in this field will pave the way for mRNA therapies to offer new hope for a wider range of diseases.

Author contributions

YT and HD conceived the concept of this review. YT prepared the original draft, and all authors contributed to the review and editing of the final manuscript.

Conflicts of interest

There are no conflicts to declare.

Data availability

This review summarizes results that have been reported previously. No primary research data, software or code have been included, and no new data were presented or analysed as part of this review. All referenced studies have been properly cited, and the intellectual property of the original authors has been respected.

Acknowledgements

This work was financially supported by Ministry of Education, Singapore (RG25/23 and MOE-T2EP30221-0019).

References

1 H. Zogg, R. Singh and S. Ro, *Int. J. Mol. Sci.*, 2022, **23**, 2736.
2 K. Horodecka and M. Düchler, *Int. J. Mol. Sci.*, 2021, **22**, 6072.
3 G. Maruggi, C. Zhang, J. Li, J. B. Ulmer and D. Yu, *Mol. Ther.*, 2019, **27**, 757–772.
4 B. A. Sullenger and S. Nair, *Science*, 2016, **352**, 1417–1420.
5 K. A. Hajj and K. A. Whitehead, *Nat. Rev. Mater.*, 2017, **2**, 1–17.

6 S. S. Rosa, D. M. Prazeres, A. M. Azevedo and M. P. Marques, *Vaccine*, 2021, **39**, 2190–2200.
7 P. Friedhoff, O. Gimadutdinow and A. Pingoud, *Nucleic Acids Res.*, 1994, **22**, 3280–3287.
8 Y. Cui, W. Shan, M. Liu, L. Wu and Y. Huang, *J. Mater. Chem. B*, 2017, **5**, 1302–1314.
9 E. H. Pilkington, E. J. Suys, N. L. Trevaskis, A. K. Wheatley, D. Zukancic, A. Algarni, H. Al-Wassiti, T. P. Davis, C. W. Pouton and S. J. Kent, *Acta Biomater.*, 2021, **131**, 16–40.
10 P. Midoux and C. Pichon, *Expert Rev. Vaccines*, 2015, **14**, 221–234.
11 M. Karam and G. Daoud, *Asian J. Pharm. Sci.*, 2022, **17**, 491–522.
12 L. Schoenmaker, D. Witzigmann, J. A. Kulkarni, R. Verbeke, G. Kersten, W. Jiskoot and D. J. Crommelin, *Int. J. Pharm.*, 2021, **601**, 120586.
13 E. Samaridou, J. Heyes and P. Lutwyche, *Adv. Drug Delivery Rev.*, 2020, **154**, 37–63.
14 L. Xu, X. Wang, Y. Liu, G. Yang, R. J. Falconer and C.-X. Zhao, *Adv. Nanobiomed Res.*, 2022, **2**, 2100109.
15 Y. Eygeris, M. Gupta, J. Kim and G. Sahay, *Acc. Chem. Res.*, 2021, **55**, 2–12.
16 Y. Zeng, M. Shen, R. Pattipeiluhu, X. Zhou, Y. Zhang, T. Bakkum, T. H. Sharp, A. L. Boyle and A. Kros, *Nanoscale*, 2023, **15**, 15206–15218.
17 J.-B. Qiao, Q.-Q. Fan, C.-L. Zhang, J. Lee, J. Byun, L. Xing, X.-D. Gao, Y.-K. Oh and H.-L. Jiang, *J. Controlled Release*, 2020, **321**, 629–640.
18 W. Yang, L. Mixich, E. Boonstra and H. Cabral, *Adv. Healthcare Mater.*, 2023, **12**, 2202688.
19 P. Huang, H. Deng, Y. Zhou and X. Chen, *Matter*, 2022, **5**, 1670–1699.
20 D. Sun and Z.-R. Lu, *Pharm. Res.*, 2023, **40**, 27–46.
21 D. Loughrey and J. E. Dahlman, *Acc. Chem. Res.*, 2021, **55**, 13–23.
22 X. Hou, T. Zaks, R. Langer and Y. Dong, *Nat. Rev. Mater.*, 2021, **6**, 1078–1094.
23 P. Patel, N. M. Ibrahim and K. Cheng, *Trends Pharmacol. Sci.*, 2021, **42**, 448–460.
24 M. Jayaraman, S. M. Ansell, B. L. Mui, Y. K. Tam, J. Chen, X. Du, D. Butler, L. Eltepu, S. Matsuda and J. K. Narayanannair, *Angew. Chem.*, 2012, **124**, 8657–8661.
25 K. J. Hassett, K. E. Benenato, E. Jacquinet, A. Lee, A. Woods, O. Yuzhakov, S. Himansu, J. Deterling, B. M. Geilich and T. Ketova, *Mol. Ther. – Nucleic Acids*, 2019, **15**, 1–11.
26 E. De Lombaerde, X. Cui, Y. Chen, Z. Zhong, J. Deckers, G. Mencarelli, L. Opsomer, H. Wang, J. De Baere and S. Lienenklaus, *ACS Nano*, 2024, **18**, 28311–28324.
27 S. A. Dilliard, Q. Cheng and D. J. Siegwart, *Proc. Natl. Acad. Sci. U. S. A.*, 2021, **118**, e2109256118.
28 G. Tesei, Y.-W. Hsiao, A. Dabkowska, G. Grönberg, M. Yanez Arteta, D. Ulkoski, D. J. Bray, M. Trulsson, J. Ulander and M. Lund, *Proc. Natl. Acad. Sci. U. S. A.*, 2024, **121**, e2311700120.
29 R. Wang and Z.-G. Wang, *Phys. Rev. Lett.*, 2014, **112**, 136101.
30 S. Patel, N. Ashwanikumar, E. Robinson, Y. Xia, C. Mihai, J. P. Griffith III, S. Hou, A. A. Esposito, T. Ketova and K. Welsher, *Nat. Commun.*, 2020, **11**, 983.
31 S. Sabnis, E. S. Kumarasinghe, T. Salerno, C. Mihai, T. Ketova, J. J. Senn, A. Lynn, A. Bulychev, I. McFadyen and J. Chan, *Mol. Ther.*, 2018, **26**, 1509–1519.
32 M. Cornebise, E. Narayanan, Y. Xia, E. Acosta, L. Ci, H. Koch, J. Milton, S. Sabnis, T. Salerno and K. E. Benenato, *Adv. Funct. Mater.*, 2022, **32**, 2106727.
33 N. Chaudhary, L. N. Kasiewicz, A. N. Newby, M. L. Arral, S. S. Yerneni, J. R. Melamed, S. T. LoPresti, K. C. Fein, D. M. Strelkova Petersen and S. Kumar, *Nat. Biomed. Eng.*, 2024, 1–16.
34 B. Li, A. Y. Jiang, I. Raji, C. Atyeo, T. M. Raimondo, A. G. Gordon, L. H. Rhym, T. Samad, C. MacIsaac and J. Witten, *Nat. Biomed. Eng.*, 2023, 1–18.
35 L. Miao, L. Li, Y. Huang, D. Delcassian, J. Chahal, J. Han, Y. Shi, K. Sadtler, W. Gao and J. Lin, *Nat. Biotechnol.*, 2019, **37**, 1174–1185.
36 L. Xue, G. Zhao, N. Gong, X. Han, S. J. Shepherd, X. Xiong, Z. Xiao, R. Palanki, J. Xu and K. L. Swingle, *Nat. Nanotechnol.*, 2024, 1–12.
37 L. Miao, Y. Zhang and L. Huang, *Mol. Cancer*, 2021, **20**, 41.
38 S. C. Semple, A. Akinc, J. Chen, A. P. Sandhu, B. L. Mui, C. K. Cho, D. W. Sah, D. Stebbing, E. J. Crosley and E. Yaworski, *Nat. Biotechnol.*, 2010, **28**, 172–176.
39 Y. Xu, A. Golubovic, S. Xu, A. Pan and B. Li, *J. Mater. Chem. B*, 2023, **11**, 6527–6539.
40 A. Akinc, A. Zumbuehl, M. Goldberg, E. S. Leshchiner, V. Busini, N. Hossain, S. A. Bacallado, D. N. Nguyen, J. Fuller and R. Alvarez, *Nat. Biotechnol.*, 2008, **26**, 561–569.
41 J. H. Felgner, R. Kumar, C. Sridhar, C. J. Wheeler, Y. J. Tsai, R. Border, P. Ramsey, M. Martin and P. L. Felgner, *J. Biol. Chem.*, 1994, **269**, 2550–2561.
42 D. Zhi, S. Zhang, B. Wang, Y. Zhao, B. Yang and S. Yu, *Bioconjugate Chem.*, 2010, **21**, 563–577.
43 L. Miao, J. Lin, Y. Huang, L. Li, D. Delcassian, Y. Ge, Y. Shi and D. G. Anderson, *Nat. Commun.*, 2020, **11**, 2424.
44 C. Liu, Y. Jiang, W. Xue, J. Liu, Z. Wang and X. Li, *Int. J. Pharm.*, 2024, **667**, 124868.
45 K. A. Hajj, R. L. Ball, S. B. Deluty, S. R. Singh, D. Strelkova, C. M. Knapp and K. A. Whitehead, *Small*, 2019, **15**, 1805097.
46 Y. Yan, X. Liu, L. Wang, C. Wu, Q. Shuai, Y. Zhang and S. Liu, *Biomaterials*, 2023, **301**, 122279.
47 K. Hashiba, M. Taguchi, S. Sakamoto, A. Otsu, Y. Maeda, Y. Suzuki, H. Ebe, A. Okazaki, H. Harashima and Y. Sato, *Nano Lett.*, 2024, **24**, 12758–12767.
48 J. Whitley, C. Zwolinski, C. Denis, M. Maughan, L. Hayles, D. Clarke, M. Snare, H. Liao, S. Chiou and T. Marmura, *Transl. Res.*, 2022, **242**, 38–55.
49 U. Kafle, H. Q. Truong, C. T. G. Nguyen and F. Meng, *Mol. Pharm.*, 2024, **21**, 5944–5959.

50 V. Kafil and Y. Omidi, *Bioimpacts*, 2011, **1**, 23.
51 U. Laemmli, *Proc. Natl. Acad. Sci. U. S. A.*, 1975, **72**, 4288–4292.
52 H. Fang, Z. Guo, L. Lin, J. Chen, P. Sun, J. Wu, C. Xu, H. Tian and X. Chen, *J. Am. Chem. Soc.*, 2018, **140**, 11992–12000.
53 T.-i. Kim, H. J. Seo, J. S. Choi, H.-S. Jang, J.-u. Baek, K. Kim and J.-S. Park, *Biomacromolecules*, 2004, **5**, 2487–2492.
54 J. Shi, H. Yin, Q. Sun, R. Teng, Y. Zhu and J. Du, *Chem. Mater.*, 2024, **36**, 5422–5435.
55 T. Miyazaki, S. Uchida, S. Nagatoishi, K. Koji, T. Hong, S. Fukushima, K. Tsumoto, K. Ishihara, K. Kataoka and H. Cabral, *Adv. Healthcare Mater.*, 2020, **9**, 2000538.
56 Z. Li, L. Amaya, R. Pi, S. K. Wang, A. Ranjan, R. M. Waymouth, C. A. Blish, H. Y. Chang and P. A. Wender, *Nat. Commun.*, 2023, **14**, 6983.
57 P. S. Kowalski, U. Capasso Palmiero, Y. Huang, A. Rudra, R. Langer and D. G. Anderson, *Adv. Mater.*, 2018, **30**, 1801151.
58 K. Shin, H.-W. Suh, A. Suberi, C.-H. Whang, M. Ene, J. Grundler, M. K. Grun and W. M. Saltzman, *Biomaterials*, 2024, **311**, 122692.
59 P. Huang, L. Jiang, H. Pan, L. Ding, B. Zhou, M. Zhao, J. Zou, B. Li, M. Qi and H. Deng, *Adv. Mater.*, 2023, **35**, 2207471.
60 D. Zhang, E. N. Atochina-Vasserman, D. S. Maurya, M. Liu, Q. Xiao, J. Lu, G. Lauri, N. Ona, E. K. Reagan and H. Ni, *J. Am. Chem. Soc.*, 2021, **143**, 17975–17982.
61 M. Yuan, Z. Han, Y. Liang, Y. Sun, B. He, W. Chen and F. Li, *Biomater. Res.*, 2023, **27**, 90.
62 L. Rotolo, D. Vanover, N. C. Bruno, H. E. Peck, C. Zurla, J. Murray, R. K. Noel, L. O'Farrell, M. Araínga and N. Orr-Burks, *Nat. Mater.*, 2023, **22**, 369–379.
63 S. He, J. Gui, K. Xiong, M. Chen, H. Gao and Y. Fu, *J. Nanobiotechnol.*, 2022, **20**, 101.
64 Y. Huang, J. Wu, S. Li, Z. Liu, Z. Li, B. Zhou and B. Li, *Theranostics*, 2024, **14**, 830.
65 M. Li, S. Li, Y. Huang, H. Chen, S. Zhang, Z. Zhang, W. Wu, X. Zeng, B. Zhou and B. Li, *Adv. Mater.*, 2021, **33**, 2101707.
66 G. Zeng, Z. He, H. Yang, Z. Gao, X. Ge, L. Liu, Z. Liu and Y. Chen, *ACS Appl. Mater. Interfaces*, 2024, **16**, 25698–25709.
67 L. M. Kranz, M. Diken, H. Haas, S. Kreiter, C. Loquai, K. C. Reuter, M. Meng, D. Fritz, F. Vascotto and H. Hefesha, *Nature*, 2016, **534**, 396–401.
68 A. Kosmides, R. Meyer, J. Hickey, K. Aje, K. Cheung, J. Green and J. Schneck, *Biomaterials*, 2017, **118**, 16–26.
69 M. Qiu, Y. Tang, J. Chen, R. Muriph, Z. Ye, C. Huang, J. Evans, E. P. Henske and Q. Xu, *Proc. Natl. Acad. Sci. U. S. A.*, 2022, **119**, e2116271119.
70 H. Yin, R. L. Kanasty, A. A. Eltoukhy, A. J. Vegas, J. R. Dorkin and D. G. Anderson, *Nat. Rev. Genet.*, 2014, **15**, 541–555.
71 N. D. Le, B. L. Nguyen, B. R. Patil, H. Chun, S. Kim, T. O. O. Nguyen, S. Mishra, S. Tandukar, J.-H. Chang and D. Y. Kim, *ACS Nano*, 2024, **18**, 8392–8410.
72 E. W. Kavanagh, S. Y. Tzeng, N. Sharma, G. R. Cutting and J. J. Green, *Biomaterials*, 2025, **313**, 122753.
73 Y. Rui, D. R. Wilson, S. Y. Tzeng, H. M. Yamagata, D. Sudhakar, M. Conge, C. A. Berlinicke, D. J. Zack, A. Tuesca and J. J. Green, *Sci. Adv.*, 2022, **8**, eabk2855.
74 H. Parhiz, V. V. Shuvaev, N. Pardi, M. Khoshnejad, R. Y. Kiseleva, J. S. Brenner, T. Uhler, S. Tuyishime, B. L. Mui and Y. K. Tam, *J. Controlled Release*, 2018, **291**, 106–115.
75 M. R. Soto, M. M. Lewis, J. Leal, Y. Pan, R. P. Mohanty, A. Veyssi, E. Y. Maier, B. J. Heiser and D. Ghosh, *Mol. Ther. – Nucleic Acids*, 2024, **35**, 102375.
76 G. Osman, J. Rodriguez, S. Y. Chan, J. Chisholm, G. Duncan, N. Kim, A. L. Tatler, K. M. Shakesheff, J. Hanes and J. S. Suk, *J. Controlled Release*, 2018, **285**, 35–45.
77 A. Schudel, D. M. Francis and S. N. Thomas, *Nat. Rev. Mater.*, 2019, **4**, 415–428.
78 S. Nie, B. Yang, R. Ma, L. Zha, Y. Qin, L. Ou, X. Chen and L. Li, *Biomaterials*, 2024, 122859.
79 A. Heine, S. Juranek and P. Brossart, *Mol. Cancer*, 2021, **20**, 1–20.
80 F. Liang and K. Loré, *Clin. Transl. Immunology*, 2016, **5**, e74.
81 E. J. Sayour, G. De Leon, C. Pham, A. Grippin, H. Kemeny, J. Chua, J. Huang, J. H. Sampson, L. Sanchez-Perez and C. Flores, *OncoImmunology*, 2017, **6**, e1256527.
82 K. Broos, K. Van der Jeught, J. Puttemans, C. Goyvaerts, C. Heirman, H. Dewitte, R. Verbeke, I. Lentacker, K. Thielemans and K. Breckpot, *Mol. Ther. – Nucleic Acids*, 2016, **5**, e326.
83 M. Aldén, F. Olofsson Falla, D. Yang, M. Barghouth, C. Luan, M. Rasmussen and Y. De Marinis, *Curr. Issues Mol. Biol.*, 2022, **44**, 1115–1126.
84 S. Liu, X. Wang, X. Yu, Q. Cheng, L. T. Johnson, S. Chatterjee, D. Zhang, S. M. Lee, Y. Sun and T.-C. Lin, *J. Am. Chem. Soc.*, 2021, **143**, 21321–21330.
85 H. Zhao, S. Ma, Y. Qi, Y. Gao, Y. Zhang, M. Li, J. Chen, W. Song and X. Chen, *Mater. Horiz.*, 2024, **11**, 2739–2748.
86 X. Zhao, J. Chen, M. Qiu, Y. Li, Z. Glass and Q. Xu, *Angew. Chem., Int. Ed.*, 2020, **59**, 20083–20089.
87 H. Ni, M. Z. Hatit, K. Zhao, D. Loughrey, M. P. Lokugamage, H. E. Peck, A. D. Cid, A. Muralidharan, Y. Kim and P. J. Santangelo, *Nat. Commun.*, 2022, **13**, 4766.
88 X. Zhang, K. Su, S. Wu, L. Lin, S. He, X. Yan, L. Shi and S. Liu, *Angew. Chem., Int. Ed.*, 2024, e202405444.
89 E. Ben-Akiva, J. Karlsson, S. Hemmati, H. Yu, S. Y. Tzeng, D. M. Pardoll and J. J. Green, *Proc. Natl. Acad. Sci. U. S. A.*, 2023, **120**, e2301606120.
90 Y. Ren, L. Zeng, Y. Tang, J. Liao, M. Jiang, X. Cao, H. Fan and J. Chen, *J. Mater. Chem. B*, 2024, **12**, 8062–8066.
91 J. De Vrieze, A. P. Baptista, L. Nuhn, S. Van Herck, K. Deswarte, H. Yu, B. N. Lambrecht and B. G. De Geest, *Adv. Ther.*, 2021, **4**, 2100079.
92 H. Liu, K. D. Moynihan, Y. Zheng, G. L. Szeto, A. V. Li, B. Huang, D. S. Van Egeren, C. Park and D. J. Irvine, *Nature*, 2014, **507**, 519–522.

93 J. De Vrieze, B. Louage, K. Deswarte, Z. Zhong, R. De Coen, S. Van Herck, L. Nuhn, C. Kaas Frich, A. N. Zelikin and S. Lienenklaus, *Angew. Chem., Int. Ed.*, 2019, **58**, 15390–15395.
94 R. Birge, S. Boeltz, S. Kumar, J. Carlson, J. Wanderley, D. Calianese, M. Barcinski, R. Brekken, X. Huang and J. Hutchins, *Cell Death Differ.*, 2016, **23**, 962–978.
95 M. B. Naeini, V. Bianconi, M. Pirro and A. Sahebkar, *Cell. Mol. Biol. Lett.*, 2020, **25**, 1–17.
96 S. Luozhong, Z. Yuan, T. Sarmiento, Y. Chen, W. Gu, C. McCurdy, W. Gao, R. Li, S. Wilkens and S. Jiang, *Nano Lett.*, 2022, **22**, 8304–8311.
97 M. Gomi, Y. Sakurai, M. Sato, H. Tanaka, Y. Miyatake, K. Fujiwara, M. Watanabe, S. Shuto, Y. Nakai and K. Tange, *Adv. Healthcare Mater.*, 2023, **12**, 2202528.
98 Q. Chen, M. Gao, Z. Li, Y. Xiao, X. Bai, K. O. Boakye-Yiadom, X. Xu and X.-Q. Zhang, *J. Controlled Release*, 2020, **323**, 179–190.
99 C.-Y. Fan, S.-W. Wang, C. Chung, J.-Y. Chen, C.-Y. Chang, Y.-C. Chen, T.-L. Hsu, T.-J. R. Cheng and C.-H. Wong, *Chem. Sci.*, 2024, **15**, 11626–11632.
100 T. B. Geijtenbeek and S. I. Gringhuis, *Nat. Rev. Immunol.*, 2016, **16**, 433–448.
101 F. C. McLean and A. M. Budy, *Annu. Rev. Physiol.*, 1959, **21**, 69–90.
102 C. Klein, A. Driessen, K. De Groot and A. Van Den Hooff, *J. Biomed. Mater. Res.*, 1983, **17**, 769–784.
103 P. I. Croucher, M. M. McDonald and T. J. Martin, *Nat. Rev. Cancer*, 2016, **16**, 373–386.
104 L. C. Hofbauer, A. Bozec, M. Rauner, F. Jakob, S. Perner and K. Pantel, *Nat. Rev. Clin. Oncol.*, 2021, **18**, 488–505.
105 I. McCarthy, *J. Bone Jt. Surg.*, 2006, **88**, 4–9.
106 B. Pf, Handbook of Experimental Pharmacology, 1988, vol. 83.
107 K. B. Farrell, A. Karpeisky, D. H. Thamm and S. Zinnen, *Bone Rep.*, 2018, **9**, 47–60.
108 L. Xue, N. Gong, S. J. Shepherd, X. Xiong, X. Liao, X. Han, G. Zhao, C. Song, X. Huang and H. Zhang, *J. Am. Chem. Soc.*, 2022, **144**, 9926–9937.
109 M. J. Mitchell, I.-C. Yoon, L. Xue, Q. Chen, J. Liu, J. Xu, Z. Siddiqui, D. Kim, B. Chen and Q. Shi, *Angew. Chem., Int. Ed.*, 2025, **64**, e202415389.
110 D. Song, Y. Zhao, Z. Wang and Q. Xu, *Adv. Mater.*, 2024, **36**, 2401445.
111 T. Oguma, T. Kanazawa, Y. K. Kaneko, R. Sato, M. Serizawa, A. Ooka, M. Yamaguchi, T. Ishikawa and H. Kondo, *J. Controlled Release*, 2024, **373**, 917–928.
112 I. Isaac, L. Patel, N. Tran, A. Singam, P. Guha, S. Park and C. Bhattacharya, *bioRxiv*, 2024, preprint, 2024.2010.2030.621163.
113 O. A. Marcos-Contreras, C. F. Greineder, R. Y. Kiseleva, H. Parhiz, L. R. Walsh, V. Zuluaga-Ramirez, J. W. Myerson, E. D. Hood, C. H. Villa and I. Tombacz, *Proc. Natl. Acad. Sci. U. S. A.*, 2020, **117**, 3405–3414.
114 E. L. Han, S. Tang, D. Kim, A. M. Murray, K. L. Swingle, A. G. Hamilton, K. Mrksich, M. S. Padilla, R. Palanki and J. J. Li, *Nano Lett.*, 2024, **25**, 800–810.
115 M. Gao, Y. Li, W. Ho, C. Chen, Q. Chen, F. Li, M. Tang, Q. Fan, J. Wan and W. Yu, *ACS Nano*, 2024, **18**, 3260–3275.
116 S. Kumar, L. E. Fry, J.-H. Wang, K. R. Martin, A. W. Hewitt, F. K. Chen and G.-S. Liu, *Prog. Retinal Eye Res.*, 2023, **92**, 101110.
117 W. Yu and Z. Wu, *Adv. Drug Delivery Rev.*, 2021, **168**, 181–195.
118 Y. Eygeris, M. Gupta, J. Kim, A. Jozic, M. Gautam, J. Renner, D. Nelson, E. Bloom, A. Tuttle and J. Stoddard, *Proc. Natl. Acad. Sci. U. S. A.*, 2024, **121**, e2307813120.
119 M. Herrera-Barrera, R. C. Ryals, M. Gautam, A. Jozic, M. Landry, T. Korzun, M. Gupta, C. Acosta, J. Stoddard and R. Reynaga, *Sci. Adv.*, 2023, **9**, eadd4623.
120 Q. Cheng, T. Wei, L. Farbiak, L. T. Johnson, S. A. Dilliard and D. J. Siegwart, *Nat. Nanotechnol.*, 2020, **15**, 313–320.
121 F. Sebastiani, M. Yanez Arteta, M. Lerche, L. Porcar, C. Lang, R. A. Bragg, C. S. Elmore, V. R. Krishnamurthy, R. A. Russell and T. Darwish, *ACS Nano*, 2021, **15**, 6709–6722.
122 Z. Luo, Y. Lin, Y. Meng, M. Li, H. Ren, H. Shi, Q. Cheng and T. Wei, *ACS Nano*, 2024, **18**, 30701–30715.
123 S. T. LoPresti, M. L. Arral, N. Chaudhary and K. A. Whitehead, *J. Controlled Release*, 2022, **345**, 819–831.
124 K. Su, L. Shi, T. Sheng, X. Yan, L. Lin, C. Meng, S. Wu, Y. Chen, Y. Zhang and C. Wang, *Nat. Commun.*, 2024, **15**, 5659.
125 H. Zhou, D. S. Chen, C. J. Hu, X. Hong, J. Shi and Y. Xiao, *Adv. Sci.*, 2023, **10**, 2303597.
126 M. Sun, K. Wang and D. Oupický, *Adv. Healthcare Mater.*, 2018, **7**, 1701070.
127 Y. Lu, A. A. Aimetti, R. Langer and Z. Gu, *Nat. Rev. Mater.*, 2016, **2**, 1–17.
128 Y. Liu, C.-F. Xu, S. Iqbal, X.-Z. Yang and J. Wang, *Adv. Drug Delivery Rev.*, 2017, **115**, 98–114.
129 B. Chen, W. Dai, B. He, H. Zhang, X. Wang, Y. Wang and Q. Zhang, *Theranostics*, 2017, **7**, 538.
130 X. Yang, Z. Pan, M. R. Choudhury, Z. Yuan, A. Anifowose, B. Yu, W. Wang and B. Wang, *Med. Res. Rev.*, 2020, **40**, 2682–2713.
131 S. Zhao, K. Gao, H. Han, M. Stenzel, B. Yin, H. Song, A. Lawanprasert, J. E. Nielsen, R. Sharma and O. H. Arogundade, *Nat. Nanotechnol.*, 2024, 1–10.
132 S. Müller, T. Fritz, M. Gimnich, M. Worm, M. Helm and H. Frey, *Polym. Chem.*, 2016, **7**, 6257–6268.
133 T. H. Cheung, A. Fuchs and M. S. Shoichet, *Adv. Funct. Mater.*, 2024, 2413220.
134 W. Cai, T. Luo, L. Mao and M. Wang, *Angew. Chem.*, 2021, **133**, 8679–8689.
135 Z. Chen, Y. Tian, J. Yang, F. Wu, S. Liu, W. Cao, W. Xu, T. Hu, D. J. Siegwart and H. Xiong, *J. Am. Chem. Soc.*, 2023, **145**, 24302–24314.
136 S. Wang, Y. Zhang, Y. Zhong, Y. Xue, Z. Liu, C. Wang, D. D. Kang, H. Li, X. Hou and M. Tian, *Proc. Natl. Acad. Sci. U. S. A.*, 2024, **121**, e2322935121.
137 L. Dong, X. Deng, Y. Li, X. Zhu, M. Shu, J. Chen, H. Luo, K. An, M. Cheng and P. Zhang, *J. Am. Chem. Soc.*, 2024, **146**, 19218–19228.

138 R. Zhang, S. Shao, Y. Piao, J. Xiang, X. Wei, Z. Zhang, Z. Zhou, J. Tang, N. Qiu and X. Xu, *Adv. Mater.*, 2023, **35**, 2303614.
139 N. Pardi, M. J. Hogan, F. W. Porter and D. Weissman, *Nat. Rev. Drug Discovery*, 2018, **17**, 261–279.
140 S. Jain, A. Venkataraman, M. E. Wechsler and N. A. Peppas, *Adv. Drug Delivery Rev.*, 2021, **179**, 114000.
141 U. Sahin, K. Karikó and Ö. Türeci, *Nat. Rev. Drug Discovery*, 2014, **13**, 759–780.
142 Z. Deng, Y. Tian, J. Song, G. An and P. Yang, *Front. Immunol.*, 2022, **13**, 887125.
143 Y. Suzuki and H. Ishihara, *Drug Metab. Pharmacokinet.*, 2021, **41**, 100424.
144 J. Di, Z. Du, K. Wu, S. Jin, X. Wang, T. Li and Y. Xu, *Pharm. Res.*, 2022, **39**, 105–114.
145 J. Chen, Z. Ye, C. Huang, M. Qiu, D. Song, Y. Li and Q. Xu, *Proc. Natl. Acad. Sci. U. S. A.*, 2022, **119**, e2207841119.
146 J. Chen, J. Chen and Q. Xu, *Annu. Rev. Biomed. Eng.*, 2022, **24**, 85–109.
147 T. Vavilis, E. Stamoula, A. Ainatzoglou, A. Sachinidis, M. Lamprinou, I. Dardalas and I. S. Vizirianakis, *Pharmaceutics*, 2023, **15**, 166.
148 E. Tambuyzer, B. Vandendriessche, C. P. Austin, P. J. Brooks, K. Larsson, K. I. Miller Needleman, J. Valentine, K. Davies, S. C. Groft and R. Preti, *Nat. Rev. Drug Discovery*, 2020, **19**, 93–111.
149 J. A. Gorzelany and M. P. de Souza, *Sci. Transl. Med.*, 2013, **5**, 178fs110.
150 H.-H. Wei, L. Zheng and Z. Wang, *Fundam. Res.*, 2023, **3**, 749–759.
151 Y. Liu, D. Zhang, Y. An, Y. Sun, J. Li, M. Zheng, Y. Zou and B. Shi, *Nano Today*, 2023, **49**, 101790.
152 R. M. Conry, A. F. LoBuglio, M. Wright, L. Sumerel, M. J. Pike, F. Johanning, R. Benjamin, D. Lu and D. T. Curiel, *Cancer Res.*, 1995, **55**, 1397–1400.
153 Y. Kim, J. Choi, E. H. Kim, W. Park, H. Jang, Y. Jang, S. G. Chi, D. H. Kweon, K. Lee and S. H. Kim, *Adv. Sci.*, 2024, 2309917.
154 M. Asmamaw and B. Zawdie, *Biol.: Targets Ther.*, 2021, 353–361.
155 F. Jiang and J. A. Doudna, *Annu. Rev. Biophys.*, 2017, **46**, 505–529.
156 J. Popovitz, R. Sharma, R. Hoshyar, B. S. Kim, N. Murthy and K. Lee, *Adv. Drug Delivery Rev.*, 2023, 115026.
157 T. Wei, Y. Sun, Q. Cheng, S. Chatterjee, Z. Traylor, L. T. Johnson, M. L. Coquelin, J. Wang, M. J. Torres and X. Lian, *Nat. Commun.*, 2023, **14**, 7322.
158 Y. Sun, S. Chatterjee, X. Lian, Z. Traylor, S. R. Sattiraju, Y. Xiao, S. A. Dilliard, Y.-C. Sung, M. Kim and S. M. Lee, *Science*, 2024, **384**, 1196–1202.
159 H. Liao, J. Liao, L. Zeng, X. Cao, H. Fan and J. Chen, *Wiley Interdiscip. Rev.: Nanomed. Nanobiotechnol.*, 2024, **16**, e2004.
160 K. Paunovska, C. D. Sago, C. M. Monaco, W. H. Hudson, M. G. Castro, T. G. Rudoltz, S. Kalathoor, D. A. Vanover, P. J. Santangelo and R. Ahmed, *Nano Lett.*, 2018, **18**, 2148–2157.
161 B. Li, I. O. Raji, A. G. Gordon, L. Sun, T. M. Raimondo, F. A. Oladimeji, A. Y. Jiang, A. Varley, R. S. Langer and D. G. Anderson, *Nat. Mater.*, 2024, 1–7.
162 P. P. Guimaraes, R. Zhang, R. Spektor, M. Tan, A. Chung, M. M. Billingsley, R. El-Mayta, R. S. Riley, L. Wang and J. M. Wilson, *J. Controlled Release*, 2019, **316**, 404–417.
163 J. Wang, Y. Ding, K. Chong, M. Cui, Z. Cao, C. Tang, Z. Tian, Y. Hu, Y. Zhao and S. Jiang, *Vaccines*, 2024, **12**, 1148.